frontiers in Immunology

REVIEW
published: 08 July 2021
doi: 10.3389/fimmu.2021.697588

TIRAP in the Mechanism of Inflammation

Sajjan Rajpoot[1], Kishore K. Wary[2], Rachel Ibbott[3], Dongfang Liu[4,5,6], Uzma Saqib[7], Teresa L. M. Thurston[3] and Mirza S. Baig[1]**

[1] Department of Biosciences and Biomedical Engineering (BSBE), Indian Institute of Technology Indore (IITI), Indore, India, [2] Department of Pharmacology and Regenerative Medicine, The University of Illinois at Chicago, Chicago, IL, United States, [3] MRC Centre for Molecular Bacteriology and Infection, Imperial College London, London, United Kingdom, [4] Department of Pathology, Immunology and Laboratory Medicine, Rutgers University-New Jersey Medical School, Newark, NJ, United States, [5] School of Graduate Studies, Rutgers Biomedical and Health Sciences, Newark, NJ, United States, [6] Center for Immunity and Inflammation, New Jersey Medical School, Rutgers-The State University of New Jersey, Newark, NJ, United States, [7] Discipline of Chemistry, Indian Institute of Technology Indore (IITI), Indore, India

OPEN ACCESS

Edited by:
You-Me Kim,
Korea Advanced Institute of Science and Technology, South Korea

Reviewed by:
Hiroyuki Oshiumi,
Kumamoto University, Japan
Joo Young Lee,
Catholic University of Korea, South Korea

***Correspondence:**
Teresa L. M. Thurston
t.thurston@imperial.ac.uk
Mirza S. Baig
msb.iit@iiti.ac.in

Specialty section:
This article was submitted to Inflammation, a section of the journal Frontiers in Immunology

Received: 19 April 2021
Accepted: 23 June 2021
Published: 08 July 2021

Citation:
Rajpoot S, Wary KK, Ibbott R, Liu D, Saqib U, Thurston TLM and Baig MS (2021) TIRAP in the Mechanism of Inflammation. Front. Immunol. 12:697588. doi: 10.3389/fimmu.2021.697588

The Toll-interleukin-1 Receptor (TIR) domain-containing adaptor protein (TIRAP) represents a key intracellular signalling molecule regulating diverse immune responses. Its capacity to function as an adaptor molecule has been widely investigated in relation to Toll-like Receptor (TLR)-mediated innate immune signalling. Since the discovery of TIRAP in 2001, initial studies were mainly focused on its role as an adaptor protein that couples Myeloid differentiation factor 88 (MyD88) with TLRs, to activate MyD88-dependent TLRs signalling. Subsequent studies delineated TIRAP's role as a transducer of signalling events through its interaction with non-TLR signalling mediators. Indeed, the ability of TIRAP to interact with an array of intracellular signalling mediators suggests its central role in various immune responses. Therefore, continued studies that elucidate the molecular basis of various TIRAP-protein interactions and how they affect the signalling magnitude, should provide key information on the inflammatory disease mechanisms. This review summarizes the TIRAP recruitment to activated receptors and discusses the mechanism of interactions in relation to the signalling that precede acute and chronic inflammatory diseases. Furthermore, we highlighted the significance of TIRAP-TIR domain containing binding sites for several intracellular inflammatory signalling molecules. Collectively, we discuss the importance of the TIR domain in TIRAP as a key interface involved in protein interactions which could hence serve as a therapeutic target to dampen the extent of acute and chronic inflammatory conditions.

Keywords: inflammation, TLR signaling, inflammatory disease, TIRAP (TIR domain-containing adaptor protein), protein-protein interaction (PPI)

INTRODUCTION

TIRAP, also known as MyD88-adaptor Like (MAL), is an adapter molecule associated with receptor-mediated activation of host immune signaling (1, 2). The innate immune system recognizes microbial pathogens through receptors, including Toll-like receptors (TLRs), which identify pathogen-associated molecular patterns (PAMP) (3, 4). Upon ligation of most TLRs with their respective ligands (PAMP), MyD88 is recruited directly to the cell surface receptor intracellular domain. In the case of TLR2 and TLR4, Myd88 recruitment is indirect and occurs *via* TIRAP. This event nucleates the formation of a large signaling complex called the "Myddosome" (5–7). The resulting downstream signaling events culminate in the activation of several transcription factors that include nuclear factor κB (NF-κB) and activated protein 1 (AP1) (6, 8–10). The activation of TLR-mediated signaling pathways is critical in driving the induction of proinflammatory cytokines by immune cells and controlling host cell survival. In this way, the cell is reprogrammed to a state that helps mitigate infection. Regulated TLR activation is required for host defense activities, yet unwanted amplification of proinflammatory cytokines is detrimental to the host. Furthermore, inappropriate receptor activation can propagate the development of autoimmune diseases in individuals harboring genetic risk factors. Therefore, it is critical to understand the TLR- and TIRAP-mediated signaling mechanisms and how these pathways are regulated.

TIRAP consists of 221 amino acids, constituting two main domains (**Figure 1**); a phosphatidylinositol 4,5-bisphosphate (PIP_2) binding domain (PBD), which is responsible for targeting TIRAP to discrete regions of the plasma membrane upon Phosphatidylinositol 4-Phosphate 5-Kinase (PIP5Kα)-mediated production of PIP_2 (11, 12) and a TIR domain, which is mainly involved in protein-protein interactions with numerous inflammatory-related proteins (6, 13, 14).

This review discusses the diverse TIRAP protein interacting partners (summarized in **Table 1**) and the significance of these during inflammatory signaling pathways and the onset of inflammatory diseases. First, we summarized the mechanism of recruitment of TIRAP; thereafter, we discuss the downstream interactions that mediate inflammatory signaling. In that respect, the **Figure 2** is mainly summarized to provide the insight of inflammatory signaling pathways mediated *via* multiple TIRAP interactions eventually leading to the activation of major transcription factors NF-κB and AP-1 and hence expression of proinflammatory cytokines (2, 9, 16, 20, 26, 29, 30, 32, 40, 41). On the other hand, the negative regulators of TIRAP interacting proteins are discussed and represented for their known roles (18, 22, 23, 35, 42).

TIRAP AND BRUTON'S TYROSINE KINASE (BTK)

For TIRAP to carry out its function as a TLR adaptor protein in inflammatory signaling, it must be recruited to the membranes' activated receptors. This occurs upon binding to PIP_2 before its interaction with TLRs (12). Subsequent interaction with TLRs' TIR domain is facilitated by tyrosine phosphorylation of selected TLRs and their adaptor molecules by several tyrosine kinases, including Bruton's tyrosine kinase (BTK), Src, Lyn, Syk, etc (43, 44). For example, phosphorylation of the cytoplasmic tail of the TLR4 TIR domain at Y674 and Y680 and phosphorylation of TIRAP tyrosine residues at positions 86, 106, 159, and 187 by BTK are required for TLR4-TIRAP-MyD88 interaction and activation of NF-κB and MAPK (mitogen-activated protein kinase) signaling leading to proinflammatory responses (**Figure 2**) (17, 26, 45, 46). BTK interaction with TIRAP and its tyrosine phosphorylation in the TIR domain is crucial for TIRAP to function. Six conserved tyrosine (Y) residues in the TIR domain of human TIRAP are the potential phosphor-acceptor site. The four residues Y86, Y106, Y159 and Y187 in TIRAP are experimentally identified as the sites for BTK mediated phosphorylation. Meanwhile, the mutation of these tyrosine residues either with alanine or phenylalanine describes them as the crucial sites for BTK mediated phosphorylation, as after stimulation, the mutation impaired the BTK association with TIRAP, similar to the previously reported P125H variant of TIRAP. Also, these mutations play a dominant negative role and impair NF-κB activation (13, 17, 26). Several studies hence concluded the significance of tyrosine sites on TIRAP in the TIR domain for association with BTK immediately on LPS stimulation. However, it is important to have a detailed understanding of the mechanism of TIRAP-BTK interaction and the role of tyrosine phosphorylation regulating the

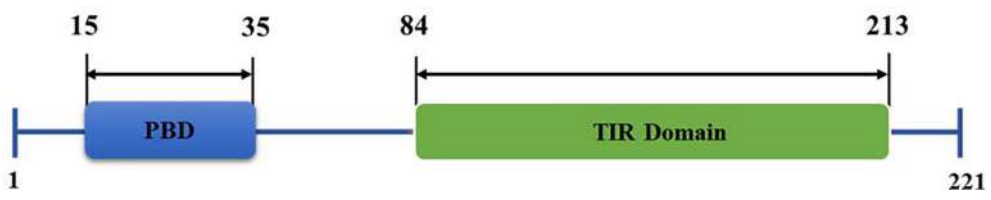

FIGURE 1 | Structural organization of Toll/interleukin 1 receptor (TIR) domain-containing adaptor protein (TIRAP) domains. The amino acid position of an N-terminal phosphatidylinositol (PI) binding domain (PBD) and a C-terminal Toll-like receptor (TIR) domain are as shown.

TABLE 1 | The significance of TIRAP interaction with the partner proteins in the cellular process.

Sr No.	Interactions	Nature of Response	Role of the Interaction in Inflammatory Pathways	References
1	TIRAP-TLR4	Pro-inflammatory response	Interaction transduces downstream signaling *via* MyD88 dependent pathway. It bridges MyD88 to TLR4 and hence activates NF-κB and AP-1 nucleus translocation and cytokines expression.	(2, 6, 8, 15)
2	TIRAP-TLR2	Proinflammatory response	As in TLR4, this interaction also bridges TRL2 to MyD88 and leads to the production of the inflammatory cytokines *via* the activation of NF-κB, AP-1, and MyD88-independent PI3k-Akt pathway.	(6, 16, 17)
3	TIRAP-MyD88	Proinflammatory response	In MyD88 dependent-pathway, the TIRAP acts as the bridging protein to bring the MyD88 to TLR4/2 inflammatory signaling.	(2, 5, 6, 8, 14, 15)
4	TIRAP-CLIP170	Inhibitory	TIRAP interacts with CLIP170 which leads to its ubiquitination and promotes proteasomal degradation resulting in reduced NF-κB and AP-1 response.	(18)
5	TIRAP-RAGE	Proinflammatory response	The stimulated RAGE receptor, similar to TLR4, binds TIRAP to activate MyD88 dependent NF-κB and AP-1 inflammatory pathways.	(19)
6	TIRAP-TRAF6	Proinflammatory response	In stimulated TLR4 pathway, the interaction leads to transactivation of p65 by its direct phosphorylation at serine-536 (p-S536) residue.	(20)
7	TIRAP-p85α	Proinflammatory response	TIRAP interacts with PI3K subunit p85α in response to the TLR2-TLR1/6 heterodimer response to activate the PI3K-Akt pathway.	(16, 21)
8	TIRAP-Triad3A	Inhibitory	In overexpressed condition, Triad3A, an E3 ubiquitin ligase interacts with TIRAP for its U&PD	(22)
9	TIRAP-SOCS1	Inhibitory	SOCS1 interacts with BTK phosphorylated TIRAP to negatively regulate it by U&PD	(23–25)
10	TIRAP-BTK	Proinflammatory response	In stimulated TLR4/2 pathways, the interaction with BTK is crucial for TIRAP activation *via* its tyrosine phosphorylation at TIR domain leading to downstream NF-κB and AP-1 activation	(17, 26–28)
11	TIRAP-PKCδ	Proinflammatory response	The interaction leads phosphorylation and activation of TIRAP which promotes the downstream p38 MAPK and NF-κB response in stimulated macrophages.	(27, 29, 30)
12	TIRAP-p38 MAPK	Proinflammatory response	The interaction leads to the activation of AP-1 and enhanced pro-inflammatory cytokine response in stimulated macrophages	(30, 31)
13	TIRAP-c-Jun	Proinflammatory response	In stimulated TLR4 pathway, this interaction leads to the transactivation of c-Jun and its nucleus translocation for proinflammatory genes expression	(32)
14	TIRAP-IRAK2	Proinflammatory response	In TLR4/2 pathway, this interaction activates NF-κB independent of MyD88 *via* TRAF6 and TAK protein leading to increased pro-inflammatory response	(2, 26)
15	TIRAP-Caspase1	Inhibitory	Caspase1 interaction leads to activation of TIRAP to increase NF-κB transcriptional activity. In a contrast study, D198E, however, function normally and hence demand more investigation.	(33, 34)
16	TIRAP-IRAK1/4	Inhibitory	In stimulated TLR4/2 pathways, TIR domain mediated interaction leads to the phosphorylation at T28 and other probable sites in TIRAP leading to its U&PD	(35)
17	TIRAP-BCAP	Inhibitory	This interaction negatively regulates TLR signaling. Dimeric BCAP interfere with the TLR-PI3K signalling and associates with TIR domain of TIRAP to negatively regulate the inflammatory response.	(36–39)

U&PD-Ubiquitination and Proteasomal degradation.

downstream signaling. The prerequisite step in the TIRAP phosphorylation by BTK is its activation itself. In stimulated macrophages, src kinase is reported to activate BTK as well as PKCδ (protein kinase C delta) (27–30, 47, 48). Structural analysis of BTK and PKCδ interaction with TIRAP suggests that Y106 of TIRAP is phosphorylated by the action of both BTK and PKCδ (27). Both phosphorylation sites promote the activation of downstream p38-MAPK, NF-κB pathways, and the associated cytokine response, but due to ubiquitin-dependent degradation of phosphorylated TIRAP mediated by SOCS1 (suppressor of cytokine signaling 1), TIRAP tyrosine phosphorylation by BTK is transient (23). With the critical molecules poised to become activated at the membrane, BTK-mediated TIRAP phosphorylation and activation, followed by degradation of phospho-TIRAP, results in a rapid yet balanced inflammatory response, avoiding prolonged TLR4 or TLR2 signaling that would otherwise result in chronic inflammation and associated diseases (23). A recently concluded study on BCR-TLR interplay suggest that the high expression of BTK in TLR signaling leads to the development of pathology in a Btk-dependent model for systemic autoimmune disease (49).

TIRAP AND RECEPTOR FOR ADVANCED GLYCATION END-PRODUCTS (RAGE)

The Receptor for advanced glycation end-products (RAGE) is a multi-ligand cell membrane receptor implicated in diverse chronic inflammatory states such as cardiovascular disease, cancer, neurodegeneration, and diabetes (50–52). RAGE is activated by diverse damage-associated molecular pattern molecules (DAMPs), which include advanced glycation end products (AGEs), high mobility group box-1 (HMGB1), and S100 proteins (51–53). Upon ligand binding, Protein Kinase C-ζ (PKC-ζ) phosphorylates the cytosolic domain of RAGE on Ser391, mediating interaction with the TIR domain TIRAP (19). As with TLR signaling, TIRAP acts as a bridge to MyD88. In this way, RAGE activation induces MyD88-dependent proinflammatory signaling (19) (**Figure 2**). The soluble RAGE is generated after either the proteolytic cleavage of its transmembrane domain to generate sRAGE or alternative splicing to give endogenous soluble RAGE (esRAGE). These proteins have distinct roles in inflammation and disease (compared to RAGE), with neither capable of inducing signaling upon binding RAGE targets. Instead, sRAGE blocks RAGE signaling effectively and

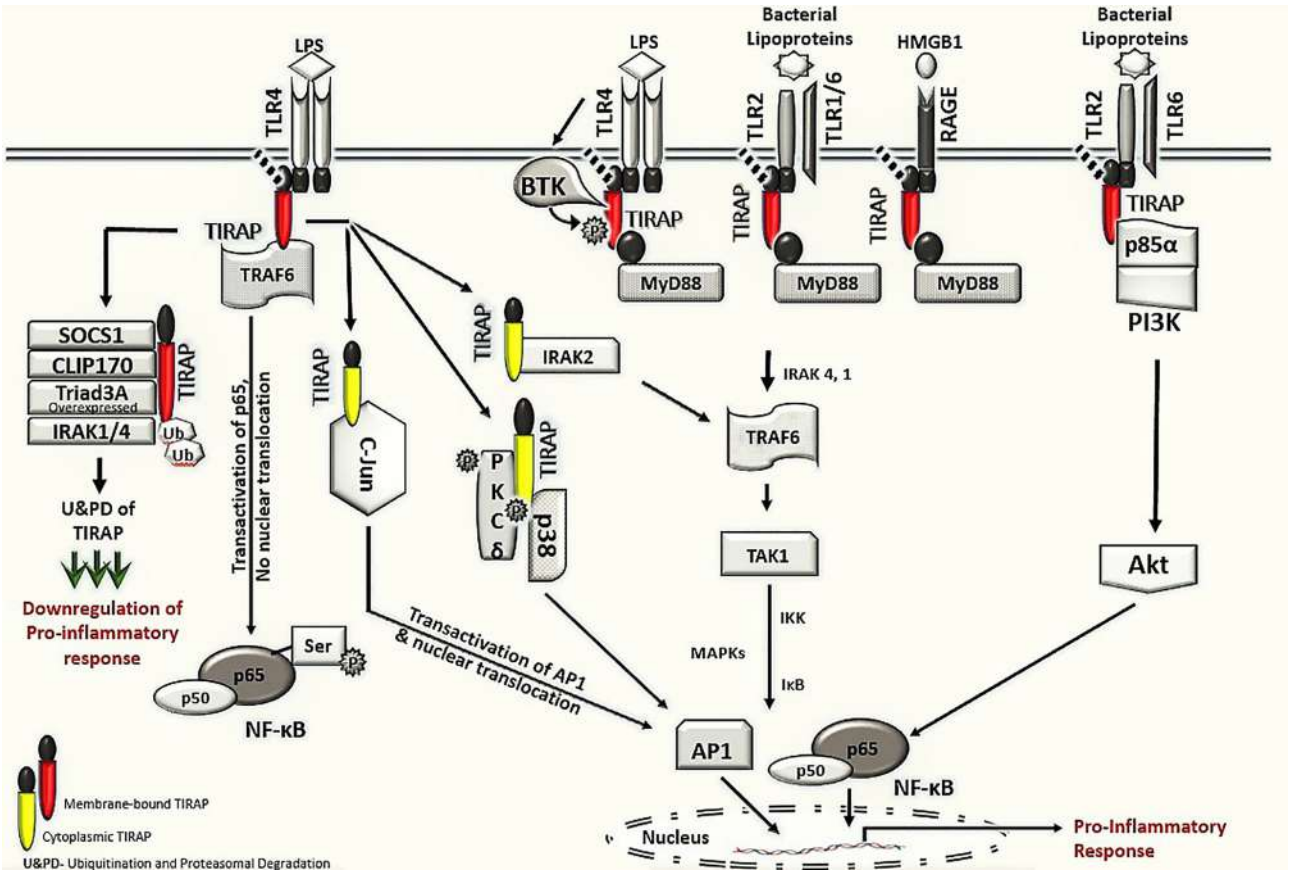

FIGURE 2 | TIRAP interacting machinery in the activation of inflammatory signaling. The membrane localized TIRAP initiates the downstream signaling via its interaction with upstream membrane bound receptors TLR4, TLR2 and RAGE as well as with membrane localized kinases BTK, p85α subunit of PI3K and BCAP. In TLR4 mediated signaling, the membrane localized TIRAP also interacts with TRAF6 for transactivation of the p65 in NF-κB pathway. The downstream inflammatory signaling *via* cytoplasmic TIRAP involves an interaction with protein kinase PKCδ and p38 MAPK as well as with IRAK2 and AP-1 subunit c-Jun, respectively. The negative regulators of TIRAP protein including SOCS1, CLIP170, IRAK1/4 and Triad3A are involved in interactions with TIRAP for its ubiquitination and proteasomal degradation (U&PD) and hence downregulation in inflammatory response mediated *via* TIRAP. TLR- Toll -interleukin-1 receptor; TIRAP- Toll-interleukin-1 Receptor (TIR) domain-containing adaptor protein; MyD88- Myeloid differentiation factor 88; RAGE- Receptor for advanced glycation end-products; BTK- Bruton's tyrosine kinase; PI3K- phosphoinositide 3-kinase; BCAP- B-cell adaptor for phosphoinositide 3-kinase; TRAF6, Tumor necrosis factor receptor (TNFR)-associated factor 6; NF-κB, Nuclear Factor kappa-light-chain-enhancer of activated B cells; PKCδ, protein kinase c delta; p38 MAPK, p38 mitogen-activated protein kinase; AP-1, Activator protein 1; SOCS1, Suppressor of cytokine signaling 1; CLIP170, Cytoplasmic linker protein 170; IRAK, interleukin-1 receptor-associated kinase; IKK, IκB kinase; and IκB, nuclear factor of kappa light polypeptide gene enhancer in B-cells inhibitor.

appear to prevent or reduce inflammatory conditions (50, 51, 54). As mutations in the TIR domain of TIRAP result in inhibition of downstream inflammatory signaling and the role of RAGE in inducing a proinflammatory immune response during disease (19). The RAGE signalling plays a vital role in many inflammatory associated diseases (acute lung injury, sepsis, inflammatory bowl disease, atherosclerosis, cancer and other chronic infectious and noninfectious diseases). Many ligands (e.g., HMGB1, s100, etc) activate both RAGE and TLR4 leading to same inflammatory pathway *via* TIRAP interaction, a direct cross talk between both signalling has also been highlighted (55, 56). It should now be explored in detail whether the therapeutic intervention of TIRAP and RAGE represents a means to treat these diseased states. An earlier study on neuronal cells has been reported to disrupt this interaction through decoy RAGE peptide (RAGE-I) targeting TIRAP and abrogates the activation of cdc42, inhibiting cell migration and invasion and protecting cell death (57).

TIRAP AND PHOSPHATIDYLINOSITOL 3′-KINASE p85 AND B-CELL ADAPTOR FOR PHOSPHOINOSITIDE 3-KINASE (BCAP)

The interaction of p85α, a regulatory subunit of phosphoinositide 3-kinase (PI3K) with TIRAP, is a MyD88-independent response of the TLR2 receptor upon stimulation with bacterial lipoproteins (16, 21). This interaction is highly significant in TLR2 and TLR6 heterodimer signaling, resulting in the activation of PI3K-

dependent phosphorylation of Akt, PIP_3 [phosphatidylinositol $(3,4,5)P_3$] generation, and polar shape changes of the macrophage (16). Signaling is initiated when TLR2 heterodimers with TLR6 are bound by diacylated lipoprotein ligands, or when TLR1/2 heterodimers are bound by triacylated lipoproteins (58). Ligand binding induces conformational changes within the receptor that bring their TIR domains close to downstream signal transduction (1, 59, 60). Upon diacylated lipoprotein stimulation of TLR2/6, TIRAP, but not MyD88, is essential for PI3K activity and NF-κB activation (16). Upon stimulation of macrophages, TIRAP interacts with p85α, and these proteins colocalize at the plasma membrane (16). Whereas MyD88 is not required for interaction of TIRAP with p85α, the efficiency of PI3K activity, and therefore downstream activation of Akt and NF-κB, as well as macrophage polarization, becomes delayed in MyD88 deficient cells (16). This suggests that the TIRAP interaction with p85α is direct but that MyD88 might accelerate the kinetics of Akt phosphorylation and PIP_3 generation.

MALP-2 induced activation of the TLR2/6 pathway in THP-1 cells also induces the interaction of TIRAP with p85α, and this is essential for the induction of Heme Oxygenase-1 (HO-1) *via* Akt phosphorylation and Nrf2 activation (21). Similar to the above study, this study also reported that MyD88 deficiency resulted in decreased Akt phosphorylation but at earlier time points post-activation (60 minutes). HO-1 expression upon MALP-2 stimulation also involves c-Src and BTK, which are other binding partners of TIRAP. These proteins are likely to form a complex consisting of c-Src, BTK, TIRAP, and p85α upon stimulation, and together, they represent a potentially important target for pharmacotherapy during various chronic inflammatory diseases.

In contrast, a multimodular protein, B-cell adaptor for phosphoinositide 3-kinase (PI3K) (BCAP) has been reported to negatively regulate the TLR4/2-PI3K signalling, suggesting its association with TLR and downstream TIR domain of TIRAP, leading to its recruitment to TLR signalasome by TIR-TIR interactions (36–38). BCAP also interacts with p85α suggesting its role in regulating the downstream signalling (36). BCAP is a dimeric protein and its oligomerization depends on its ANK (ankyrin repeat) and DBB (Dof/BANK1/BCAP) domains. A recently concluded study clearly defines the importance of DBB domain in dimerization and its role in TIRAP-BCAP interaction (39). The monomeric BCAP, though fails to negatively regulate the TLR signaling suggesting that only domain dimerization drives the negative response. The TIRAP TIR domain is reported to assemble to form filament complex *in vitro*, an event critical for signal transduction. Such a filament could be disrupted by dimeric, and not monomeric, BCAP. Another angle suggest BCAP phosphoinositide metabolism, which cleaves PIP2 to DAG and IP3 and hence deprives TIRAP for its membrane anchor required for TLR signaling (39). Overall, the BCAP association mainly with TIRAP and p85α provides novel directions for regulatory pathways in inflammation.

TIRAP AND PROTEIN KINASE C-δ (PKCδ)

As mentioned above, PKCδ represents an interacting partner of TIRAP that is required for TLR2- and TLR4-induced activation of p38 MAPK, NF-κB and proinflammatory cytokine expression (29, 30). Mice harboring PKCδ-deficiency reduces the bacterial killing function of macrophages, showing decreased NO, ROS, and H2O2, resulting in hyper-susceptible animals to infection with mycobacterium tuberculosis with increased mortality (61). Mechanistically, PKCδ constitutively interacts with and phosphorylates Y106 in the TIR domain of TIRAP as described above, and BTK phosphorylates TIRAP at Y106, as well as Y86 (27). Accordingly, Baig et al., 2017 reported a novel heterotrimeric complex consisting of TIRAP, PKCδ, and p38 MAPK required for AP1-mediated inflammatory responses in macrophages in response to LPS stimulation (30). Thus, TIRAP activity is regulated in response to receptor stimulation. In this situation, TIRAP was not required for the phosphorylation of PKCδ but was required for cytokine production (30). In summary, PKCδ activation is likely required downstream of TIRAP; however, it remains unclear how PKCδ activation is regulated in macrophages upon LPS stimulation.

TIRAP AND CYTOPLASMIC LINKER PROTEIN 170 (CLIP170)

Cytoplasmic linker protein 170 (CLIP170), containing two conserved cytoskeleton-associated protein Glycine rich (CAP-Gly) domains and two tandem repeats of zinc knuckle motifs (also called CCHC zinc fingers), is a multifunctional protein that binds to and regulates the dynamics of the growing plus end of microtubules (62–64). In addition, CLIP170 acts as a negative regulator of TLR4 by inducing TIRAP ubiquitination (both mono and polyubiquitination) and promoting its proteasomal degradation. Accordingly, this activity of CLIP170 decreased downstream signaling activity, including reduced NF-κB MAPK activity. Further, the activity of CLIP170 is specific to TIRAP, with MyD88 levels unaltered upon overexpression of CLIP170 (18). Analogous to many negative regulators, CLIP170 expression is induced upon stimulation with LPS. Interestingly, the pathogenic bacteria *Brucella* species viz. *Brucella melitensis, Brucella abortus*, and *Brucella ovis* inhibit TIRAP activity by encoding a TIR domain-containing effector protein TcpB, also called Btp1 (65). TcpB, like TIRAP, shares phosphoinositide binding properties and resemblance in its TIR domain; however, functionally, TcpB impairs TLR-4 and TLR-2 induced NF-κB activation inflammatory responses (18, 65). Mechanistically, TcpB interacts with TIRAP and promotes CLIP170-dependent polyubiquitination and subsequent proteasomal degradation of TIRAP (18). CLIP170 is also of therapeutic interest; Pregnenolone, a steroid hormone precursor, suppresses TLR4 and TLR2 mediated inflammation by promoting CLIP170-mediated ubiquitination and degradation of TIRAP (66).

TIRAP AND c-JUN

Delivery of bacterial-derived pathogenic LPS to TLR4 has been shown to activate AP-1 through a series of phosphorylation events

on serine/threonine residues mediated by upstream MAPKs (extracellular signal-regulated kinases; ERK, c-Jun N-terminal kinase; JNK, and p38 mitogen-activated protein kinases; p38 kinase) (67). For example, c-Jun, which contains a transactivation domain, is phosphorylated at Ser 63 and 73 by JNKs, resulting in its activation (67). c-Jun can form homo and heterodimers with other AP-1 family members, including c-Fos or ATF (Activating transcription factor) to make transcriptionally active complexes (68–70); (71). These transcriptionally active dimeric components of AP-1 now control the activation of critical proinflammatory cytokine genes such as TNF-α, IL-12, IL-23, and other proinflammatory cytokines (72–75). In recent findings, TIRAP was found to interact with the AP-1 subunit c-Jun in endotoxin-induced macrophages. This drives the transactivation of c-Jun, its translocation to the nucleus, and a proinflammatory immune response (32). Careful analysis of the molecular docking of a TIRAP-c-Jun crystal structure with immunoprecipitation experiments revealed the direct interaction of TIRAP with c-Jun (32). The pharmacological inhibitor Gefitinib, which abrogates the interaction of TIRAP with c-Jun, specifically reveals the importance of TIRAP-mediated c-Jun transactivation; treatment with Gefitinib drastically reduced the expression of several proinflammatory cytokines (IL-12, IL-23, TNF-α) in both bone-marrow-derived macrophages and in animals (32).

TIRAP AND p38 MITOGEN-ACTIVATED PROTEIN KINASE

As mentioned above, p38 MAPK is one of three members of the MAPK protein family, that in response to LPS, induces the expression of proinflammatory cytokines (IL-12, IL-23, TNF-α, IL-6, and IL-1β) through activation of the downstream transcription factor AP-1 (31). In addition, the MyD88-dependent TLR4/TLR2 induced activation of MAPKs and NF-κB and subsequent proinflammatory response is well characterized (3, 5, 15, 31, 76). Interestingly, this inflammatory response is also regulated through the direct interaction of TIRAP with p38 MAPK and PKCδ in LPS-stimulated macrophages (30) and suggests that TIRAP has multiple functions in the induction of MAPK signaling.

TIRAP AND CASPASE-1

Two reports on the interaction of TIRAP with Caspase-1 have highlighted the importance of this interaction to macrophage signaling events (33, 34). Caspases are evolutionarily conserved enzymes with aspartate-specific, cysteine dependent proteolytic activity, which are involved in inflammation and apoptosis (77, 78). Caspase-1, formerly called IL-1beta converting enzyme (ICE), is synthesized as a zymogen precursor and is cleaved into its p20 (20kDa) and p10 (10kDa) active catalytic subunits and a non-catalytic Caspase Activation and Recruitment Domain (CARD) (79, 80). Active caspase-1, often found in a multi-protein complex called the inflammasome, cleaves the inactive pro-forms of IL-1β and IL-18 to generate active cytokines. This function of caspase-1, as well as activation of gasdermin-D (GSDMD), is critical for the inflammatory immune response of LPS-primed macrophages (80, 81). TIRAP first found to interact with caspase-1 by yeast two-hybrid, is not required for the activation of Caspase-1 (33). Instead, caspase-1 appears to cleave TIRAP (but not MyD88), and this is required for TLR4, and TLR2 mediated NF-κB, p38 MAPK activation, and cytokine production but not IL-1 and TLR7 signaling, which is TIRAP independent (33, 34). After LPS stimulation of macrophages, caspase-1 was reported to cleave after D198 in the C-terminal region of TIRAP. However, the significance of this cleavage was questioned by another study, which found that cleavage was not required for NF-κB activity (34). Instead, it appears that mutation of D198A disrupts TLR4 mediated signaling due to the loss in the acidic amino acid at this site and not due to loss of caspase-1 cleavage. Indeed, TIRAP-D198E remained functional, suggesting that TIRAP is functional in its full-length form (34). Therefore, whether the caspase-1-TIRAP interaction is of biological relevance requires further study.

TIRAP AND TUMOR NECROSIS FACTOR RECEPTOR (TNFR)-ASSOCIATED FACTOR 6 (TRAF6)

A novel role for TIRAP in NF-κB p65 trans-activation was described after the identification that TIRAP interacts with TRAF-6 (20). The interaction following activation of TLR2 or TLR4 is direct in nature and independent of membrane localization (**Figure 2**). The TRAF family of adaptor proteins and E3 ubiquitin ligases comprises of 6 members, viz., TRAF1, TRAF2, TRAF3, TRAF4, TRAF5, and TRAF6, with each member having distinct functions in the regulation of immune signaling (82). A short motif, Pro-X-Glu-X-X-Z (X: any amino acid; Z: aromatic/acidic residue), acts as a TRAF6 binding motif that is found in various receptors and adaptor proteins (82). TIRAP contains a TRAF6 binding domain, with mutation of this motif (TIRAP-E190A), abolishing interaction with TRAF6 and preventing signal transduction (20). Functionally, the interaction of TIRAP with TRAF6 promotes serine-536 phosphorylation of the p65 subunit of NF-κB, which regulates its transcriptional activation, rather than nuclear translocation (20). In contrast, a recent study based on a mathematical data-model suggests that TIRAP-independent MyD88 activation and Myddosome complex formation in TLR4 signaling does not require TRAF6 (83).

TIRAP AND E3 UBIQUITIN-PROTEIN LIGASE RNF216 (TRIAD3A)

Triad3A is a RING finger-type E3 ubiquitin-protein ligase that recognizes and interacts with the TIR domain of TLRs,

promoting their proteolytic degradation (22, 42). Specifically, Triad3A causes K48-linked ubiquitination and degradation of TLR4 and TLR9. In addition, Fearns et al. (2006) demonstrated that overexpressed Triad3A directly interacts with and results in degradation of the TLR4 adaptor proteins TIRAP, TRIF, and RIP1 but not other adaptor proteins such as MyD88 and TRAM (22). This suggests that TIRAP is post-translationally regulated *via* different E3 ligases (CLIP170 and Triad3A). Future work should determine the relative contributions and functions to proinflammatory immune signaling.

TIRAP AND INTERLEUKIN-1 RECEPTOR-ASSOCIATED KINASE-LIKE 2 (IRAK-2)

The interleukin-1 receptor-associated kinase (IRAK) family protein kinase consists of four members, IRAK-1, IRAK-2, IRAK-3/M, and IRAK-4 (84). The sequential activation and recruitment of IRAKs, excluding IRAK-M, in MyD88 dependent signaling is well studied and reported in TLR signaling (76, 85–87). In the TLR-4-TIRAP-MyD88 mydossome complex, active MyD88 interacts with the N-terminal death domains of IRAK4, triggering a series of phosphorylation events and recruitment of IRAK-1 and IRAK-2, which are required for TRAF-6 ubiquitination, activation, and downstream activation of NF-κB (88, 89). In addition, IRAK-2, but not IRAK-1, directly interacts with TIRAP, and this results in NF-κB activation (2, 26). Further evidence for the critical role of IRAK-2 comes from the observation that a dominant-negative variant blocks TIRAP-induced NF-κB activation. The precise residues that mediate the TIRAP-IRAK-2 interaction remain unknown, but the critical tyrosine residues of TIRAP (Y86, Y106, and Y159) are not required (26). Further research is required to understand the precise physiological role of the IRAK-2-TIRAP signaling axis and test whether it represents a means for developing targeted therapeutics that control inflammation.

TIRAP AND INTERLEUKIN-1 RECEPTOR-ASSOCIATED KINASE-LIKE 1/4 (IRAK1/4)

Interestingly, the interaction of TIRAP with IRAK-4 and IRAK-1 can result in TIRAP degradation following its phosphorylation and ubiquitination, and therefore inhibition of signaling. In this way, IRAK-1/-4 negatively regulates TLR-4/2 signaling by expressing an auto-active IRAK4 inducing TIRAP degradation (35). The interaction appears to be mediated by the TIR domain of TIRAP, with mutation of proline at position 125 (P125H) in the BB loop abolishing the interaction. Both IRAK-4 and IRAK-1 phosphorylate multiple sites, including T28 on TIRAP, that are required for subsequent ubiquitination and degradation (35). Additional research is required to dissect the additional phosphorylation sites within TIRAP, as well as the ubiquitination sites that control TIRAP degradation. Furthermore, the selective role of IRAK-4 and IRAK-1 both as positive and negative regulators is an important consideration in the investigation of inflammation. It is interesting to speculate that over time IRAK-1 and IRAK-4 switch from a positive role in MyD88 dependent inflammatory signaling to a negative one, helping to dampen signaling and prevent too much inflammation. What controls this switch should be investigated using a dose-dependent endotoxin challenge over time, with careful monitoring of TIRAP complex composition.

TIRAP AND SUPPRESSOR OF CYTOKINE SIGNALING 1 (SOCS1)

The suppressor of cytokine signaling (SOCS1) serves as a key physiological regulator of both innate and adaptive immunity acting through macrophages, dendritic cells, B-cells, and T-cells (90). Structurally, the eight intracellular members of the SOCS family, SOCS1-SOCS7 and CIS, have a central SH2 domain, N-terminal extended SH2 subdomain and a variable region, and C-terminal 40 amino acid SOCS box. The SOCS box recruits factors for E3 ubiquitin ligase mediated target protein ubiquitination followed by proteasomal degradation (90, 91). Previous studies described SOCS1 as a negative intracellular regulator in the cytokine-induced JAK-STAT pathway; however, subsequent studies have addressed the role of SOCS1 that is associated with TLR4 and TLR2 signaling as an E3 ligase that polyubiquitinates TIRAP along with other proteins such as p65 and IRAK1, causing their 26S proteasomal degradation (23–25). Analogous to PEST (Proline, Glutamic acid, Serine, and Threonine) motif-containing proteins such as IκB, the PEST region of TIRAP mediates its phosphorylation, lysine polyubiquitination, and degradation, after LPS and Pam_3Cys induced TLR4 and TLR2 signaling, but not following TLR7 and TLR9. Unlike TIRAP, MyD88 does not contain a PEST domain. This degradation appears dependent on SOCS1; a mutant SOCS1 (SH2 and SOCS Box) variant, as well as SOCS1 deficient macrophages, are unable to target and degrade TIRAP in response to LPS ligation, whereas wild type SOCS1 interacted and degraded TIRAP as early as 15 to 30 minutes post LPS stimulation (23). As tyrosine phosphorylation of TIRAP is required for SOCS1-mediated degradation, it appears that TIRAP is degraded only after BTK has been activated and has phosphorylated TIRAP (23, 24). Further, the tyrosine phosphorylated TIRAP generates a binding site for SH2-domain of SOCS1 (24). Accordingly, SOCS1-mediates the negative regulation of TIRAP to prevent sustained NF-κB and MAPK activities in macrophages (23). In addition to TIRAP phosphorylation, SOCS1 functional activity also depends on NOS1-derived NO production (74, 92). In response to LPS in TLR4 signaling, NOS1 derived NO production resulted in degradation of wild-type SOCS1 post-S-nitrosation, whereas pharmacological inhibition of NOS1 resulted in increased SOCS1 expression and a concomitant increase in TIRAP degradation (74). Therefore, it will be a rewarding effort to elucidate how the NOS1 axis, propagating sustained TIRAP activation, balances with TIRAP degradation mediated *via* BTK and SOCS1 during different inflammatory events (**Figure 2**).

COMPUTATIONAL PREDICTION OF TIRAP PHOSPHORYLATION AND NITROSYLATION SITES

Studies have described the role of TIRAP in modifying the innate immune response elicited largely by endotoxin (4, 5, 9, 15, 17, 93). However, the increasing number of TIRAP partner proteins and their role in the activation of inflammatory response (**Figures 2** and **3**) pose great potential as therapeutic targets, demanding further structural elucidation. Here we have attempted to give a brief insight into the basic architecture of TIRAP and its protein-binding domain. The human TIRAP gene encodes a 221 amino

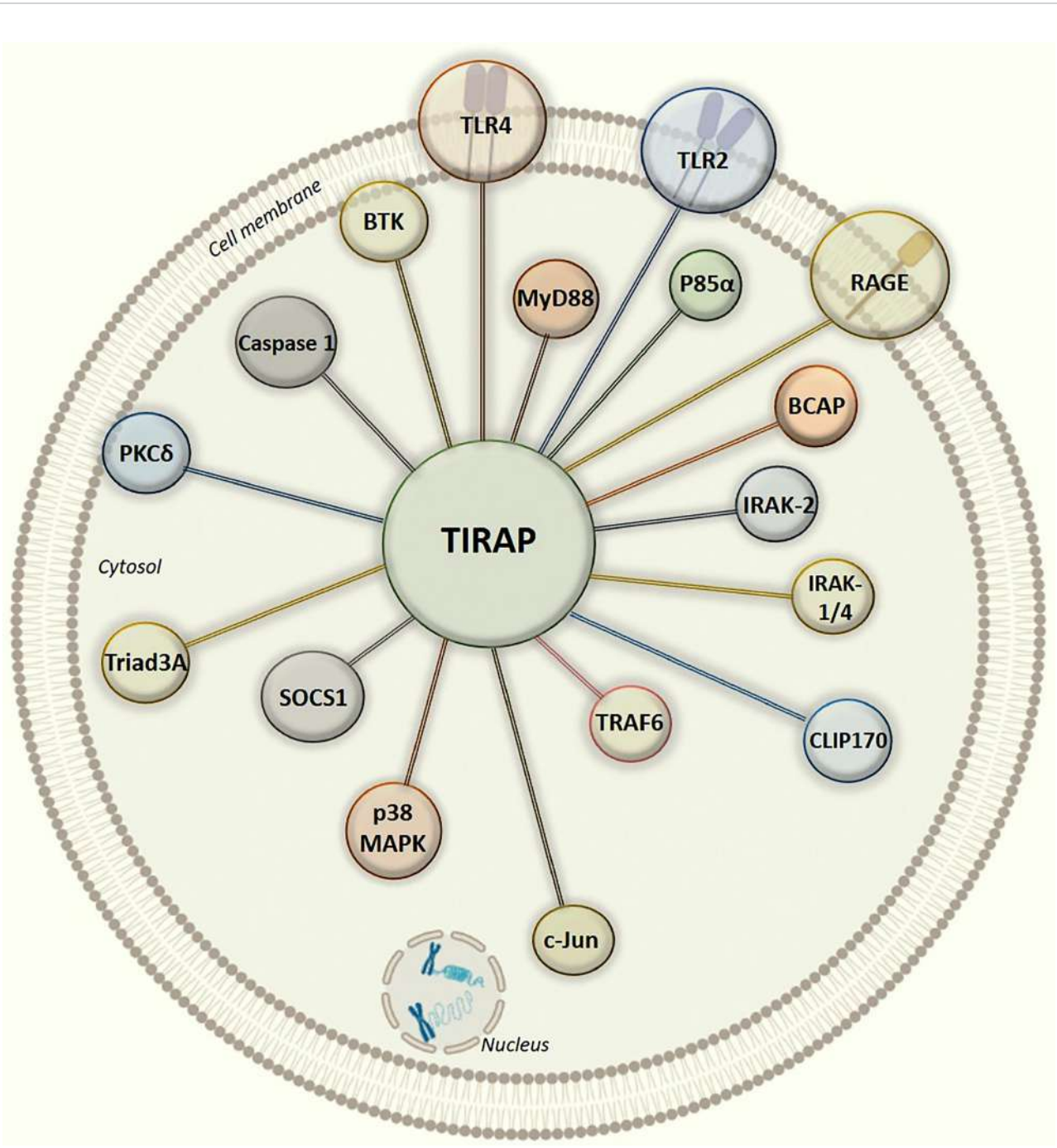

FIGURE 3 | Graphical illustration of intracellular protein-protein interaction network of TIRAP with experimentally defined partner proteins.

acid protein (10). Segregating TIRAP protein sequence gives us an N-terminal region spanning from the 1st to 83rd amino acid containing the PBD (Phosphatidylinositol 4,5-bisphosphate (PIP_2) Binding Domain) from the 15th to 35th amino acid sequence that is rich in lysine residues. A C-terminal region mainly encodes the TIR Domain, spanning for 130 amino acid long from 84th to 213th (10, 13, 94). Also, we used the Motif search tool at www.genome.jp (https://www.genome.jp/tools/motif/) to obtain the domain details from different databases as produced by the tool search results.

In all the interactions discussed above (**Figure 3**), it is interesting to note that the TIR domain is centrally involved in making interactions with the TIRAP partner proteins. Though, there may be numerous post-translational modifications which can regulate TIRAP interactions, however, the experimental evidence of tyrosine phosphorylation in the TIR domain is one of the most common and validated. Besides, the macrophages largely produce NOS (Nitric oxide synthase) mediated NO (nitric oxide) which has a crucial role in regulating inflammatory responses, for example, NOS1 protects TIRAP degradation from SOCS1 (74, 92). Unlike phosphorylation, there is no experimental evidence of NO mediated nitrosylation sites yet in TIRAP, however, we may presume that the presence of Cystine S-nitrosylation site in TIR domain may be another key factor in regulating the interaction and signaling events. However, S-glutathionylation of cysteine at C91 in TIR domain has been shown to increase the interaction of TIRAP with MyD88 (95).

Besides the known phosphorylation sites, TIR domain might also encompass other sites which might be crucial for a string of TIRAP mediated interactions. Hence, in the current review, we also attempted to computationally predict possible Serine/threonine/tyrosine phosphorylation and S-nitrosylation sites on TIRAP. Briefly, the human TIRAP TIR domain sequence retrieved from UniProt (UniProtKB- P58753) was used for the prediction and study. We searched the protein phosphorylation database PhosphoSitePlus server (https://www.phosphosite.org/homeAction) and the same sites were retrieved for human TIRAP TIR domain. Further, the predictions of possible phosphorylation sites in TIR domain were obtained from kinase-based phosphorylation prediction tools; GPS-phosphorylation (http://gps.biocuckoo.cn/) (96) and NetPhos 3.1 (http://www.cbs.dtu.dk/services/NetPhos/) (97). Including the experimentally proved sites, both the tools predicted same number of a total 21 probable phosphorylation sites (10 serine sites, 05 threonine sites, and 06 tyrosine sites) (**Supplementary Figure 1**). Similarly, the S-Nitrosylation (SNO) sites in TIR domain were predicted from three different computational tools [GPS-SNO (http://sno.biocuckoo.org) (98), DeepNitro (www.deepnitro.renlab.org) (99) and SNOSite (http://csb.cse.yzu.edu.tw/SNOSite/predict.php)] (100). Interestingly, all the SNO sites predicted from these three independent tools were found similar (**Supplementary Figure 1**). The graphical representation of TIRAP and its domains, as presented in **Supplementary Figure 1**, was further depicted using the DOG Domain illustrator tool (http://dog.biocuckoo.org/). In support of these predictions, the tyrosine residues Y86, Y106, Y159, and Y187 have been reported to be the experimentally confirmed phosphorylation sites which modulate the interaction of TIRAP with BTK protein and downstream transcription factors activation (13, 17, 26, 27).

Since the discovery of TIRAP, it has been shown to have an elaborate role in inflammatory signalling. As summarized in this review, many investigators have identified its diverse functions other than that of its role as an adaptor protein. The dynamic nature of TIRAP interaction with several upstream and downstream signaling proteins in varied inflammatory pathways draws immense curiosity towards the post-translational modifications in its TIR domain. Interestingly, a recent study described the interaction of TIRAP and MyD88 with IL1R1 (interleukin-1 receptor like-1) receptor in response to a *Helicobacter pylori* released stimuli (101). Though this study focuses on experimentally validated phosphorylation sites of TIRAP TIR domain, it would be interesting to experimentally identify novel modifications sites on TIRAP which may reveal other crucial interactions involved in signaling pathways.

CONCLUSION

The report that TIRAP acts as a second adaptor protein after MyD88 in the year 2001 was marked as a major discovery in the mechanism of TLR4-dependent inflammatory signaling. Subsequently, two more adaptor proteins, TRIF and TRAM, mostly responsible for IRF3 activation, were added to the family of TIR domain-containing adaptor proteins. More recent studies show that TIRAP not only acts as a bridging protein between TLR4/2 and MyD88, but also propagates transduction of downstream signaling events, sometimes in a MyD88-independent manner. Clearly, the ability of TIRAP to interact and collaborate with several signaling molecules in a context-dependent manner means this protein is a major regulator of cell signaling.

AUTHOR CONTRIBUTIONS

Conceptualization: MB. Investigation: MB. Writing (Original Draft): MB and SR. Reviewing and editing TT, RI, KW, US, and DL. Supervision: TT. All authors contributed to the article and approved the submitted version.

FUNDING

A Biotechnology and Biological Sciences Research Council (BBSRC) David Phillips Fellowship (BB/R011834/1) funds TLMT.

ACKNOWLEDGMENTS

The authors acknowledge the Indian Institute of Technology Indore (IITI) for providing facilities and other support. This work was supported by Cumulative Professional Development

Allowance (CPDA) from IITI to MB. The authors also acknowledge American Heart Association's (AHA) support to KW and National Institutes of Health's (NIH) support to DL.

SUPPLEMENTARY MATERIAL

The Supplementary Material for this article can be found online at: https://www.frontiersin.org/articles/10.3389/fimmu.2021.697588/full#supplementary-material

Supplementary Figure 1 | Representation of TIRAP TIR (Toll/Interleukin-1 Receptor) domain and computational prediction of serine (S), threonine (T) and tyrosine (Y) phosphorylation and cysteine (C) S-nitrosylation (SNO) positions. The TIRAP protein containing an N-terminal PBD and C-terminal TIR domain are highlighted. The predicted phosphorylation sites on top and SNO sites at bottom of domain map are indicated in blue and light brown colors, respectively. The experimentally proved phosphorylation sites (Y86, Y106, Y159, and Y187) are marked with asterisk. The predicted phosphorylation sites were obtained from kinase-based computational tools GPS-Phosphorylation (http://gps.biocuckoo.cn/) and NetPhos 3.1 (http://www.cbs.dtu.dk/services/NetPhos/). For cysteine (C) SNO sites, computational tools GPS-SNO (http://sno.biocuckoo.org/index.php), DeepNitro (www.deepnitro.renlab.org), and SNOSite (http://csb.cse.yzu.edu.tw/SNOSite/predict.php) were used.

REFERENCES

1. O'Neill LA, Bowie AG. The Family of Five: TIR-Domain-Containing Adaptors in Toll-Like Receptor Signalling. *Nat Rev Immunol* (2007) 7 (5):353–64. doi: 10.1038/nri2079
2. Fitzgerald KA, Palsson-McDermott EM, Bowie AG, Jefferies CA, Mansell AS, Brady G, et al. Mal (MyD88-Adapter-Like) Is Required for Toll-Like Receptor-4 Signal Transduction. *Nature* (2001) 413(6851):78–83. doi: 10.1038/35092578
3. Kawai T, Akira S. The Role of Pattern-Recognition Receptors in Innate Immunity: Update on Toll-Like Receptors. *Nat Immunol* (2010) 11(5):373–84. doi: 10.1038/ni.1863
4. Kawasaki T, Kawai T. Toll-Like Receptor Signaling Pathways. *Front Immunol* (2014) 5:461. doi: 10.3389/fimmu.2014.00461
5. Balka KR, De Nardo D. Understanding Early TLR Signaling Through the Myddosome. *J Leukoc Biol* (2019) 105(2):339–51. doi: 10.1002/JLB.MR0318-096R
6. Bernard NJ, O'Neill LA. Mal, More Than a Bridge to Myd88. *IUBMB Life* (2013) 65(9):777–86. doi: 10.1002/iub.1201
7. Latty SL, Sakai J, Hopkins L, Verstak B, Paramo T, Berglund NA, et al. Activation of Toll-Like Receptors Nucleates Assembly of the MyDDosome Signaling Hub. *Elife* (2018) 7:e31377. doi: 10.7554/eLife.31377
8. Lu YC, Yeh WC, Ohashi PS. LPS/TLR4 Signal Transduction Pathway. *Cytokine* (2008) 42(2):145–51. doi: 10.1016/j.cyto.2008.01.006
9. Palsson-McDermott EM, O'Neill LA. Signal Transduction by the Lipopolysaccharide Receptor, Toll-Like Receptor-4. *Immunology* (2004) 113(2):153–62. doi: 10.1111/j.1365-2567.2004.01976.x
10. Belhaouane I, Hoffmann E, Chamaillard M, Brodin P, Machelart A. Paradoxical Roles of the MAL/Tirap Adaptor in Pathologies. *Front Immunol* (2020) 11:569127. doi: 10.3389/fimmu.2020.569127
11. Kagan JC, Medzhitov R. Phosphoinositide-Mediated Adaptor Recruitment Controls Toll-Like Receptor Signaling. *Cell* (2006) 125(5):943–55. doi: 10.1016/j.cell.2006.03.047
12. Patra MC, Choi S. Insight Into Phosphatidylinositol-Dependent Membrane Localization of the Innate Immune Adaptor Protein Toll/Interleukin 1 Receptor Domain-Containing Adaptor Protein. *Front Immunol* (2018) 9:75. doi: 10.3389/fimmu.2018.00075
13. Lin Z, Lu J, Zhou W, Shen Y. Structural Insights Into TIR Domain Specificity of the Bridging Adaptor Mal in TLR4 Signaling. *PloS One* (2012) 7(4): e34202. doi: 10.1371/journal.pone.0034202
14. Ohnishi H, Tochio H, Kato Z, Orii KE, Li A, Kimura T, et al. Structural Basis for the Multiple Interactions of the MyD88 TIR Domain in TLR4 Signaling. *Proc Natl Acad Sci USA* (2009) 106(25):10260–5. doi: 10.1073/pnas.0812956106
15. Chow JC, Young DW, Golenbock DT, Christ WJ, Gusovsky F. Toll-Like Receptor-4 Mediates Lipopolysaccharide-Induced Signal Transduction. *J Biol Chem* (1999) 274(16):10689–92. doi: 10.1074/jbc.274.16.10689
16. Santos-Sierra S, Deshmukh SD, Kalnitski J, Kuenzi P, Wymann MP, Golenbock DT, et al. Mal Connects TLR2 to PI3Kinase Activation and Phagocyte Polarization. *EMBO J* (2009) 28(14):2018–27. doi: 10.1038/emboj.2009.158
17. Gray P, Dunne A, Brikos C, Jefferies CA, Doyle SL, O'Neill LA. MyD88 Adapter-Like (Mal) is Phosphorylated by Bruton's Tyrosine Kinase During TLR2 and TLR4 Signal Transduction. *JJoBC* (2006) 281(15):10489–95. doi: 10.1074/jbc.M508892200
18. Jakka P, Bhargavi B, Namani S, Murugan S, Splitter G, Radhakrishnan G. Cytoplasmic Linker Protein CLIP170 Negatively Regulates TLR4 Signaling by Targeting the TLR Adaptor Protein TIRAP. *J Immunol* (2018) 200 (2):704–14. doi: 10.4049/jimmunol.1601559
19. Sakaguchi M, Murata H, Yamamoto K, Ono T, Sakaguchi Y, Motoyama A, et al. TIRAP, an Adaptor Protein for TLR2/4, Transduces a Signal From RAGE Phosphorylated Upon Ligand Binding. *PloS One* (2011) 6(8):e23132. doi: 10.1371/journal.pone.0023132
20. Verstak B, Nagpal K, Bottomley SP, Golenbock DT, Hertzog PJ, Mansell A. MyD88 Adapter-Like (Mal)/TIRAP Interaction With TRAF6 is Critical for TLR2- and TLR4-Mediated NF-kappaB Proinflammatory Responses. *J Biol Chem* (2009) 284(36):24192–203. doi: 10.1074/jbc.M109.023044
21. You X, Liu L, Zeng Y, Li R, He J, Ma X, et al. Macrophage-Activating Lipopeptide-2 Requires Mal and PI3K for Efficient Induction of Heme Oxygenase-1. *PloS One* (2014) 9(7):e103433. doi: 10.1371/journal.pone.0103433
22. Fearns C, Pan Q, Mathison JC, Chuang TH. Triad3A Regulates Ubiquitination and Proteasomal Degradation of RIP1 Following Disruption of Hsp90 Binding. *J Biol Chem* (2006) 281(45):34592–600. doi: 10.1074/jbc.M604019200
23. Mansell A, Smith R, Doyle SL, Gray P, Fenner JE, Crack PJ, et al. Suppressor of Cytokine Signaling 1 Negatively Regulates Toll-Like Receptor Signaling by Mediating Mal Degradation. *Nat Immunol* (2006) 7(2):148–55. doi: 10.1038/ni1299
24. Fujimoto M, Naka T. SOCS1, a Negative Regulator of Cytokine Signals and TLR Responses, in Human Liver Diseases. *Gastroenterol Res Pract* (2010) 2010:470468. doi: 10.1155/2010/470468
25. Kinjyo I, Hanada T, Inagaki-Ohara K, Mori H, Aki D, Ohishi M, et al. SOCS1/JAB is a Negative Regulator of LPS-Induced Macrophage Activation. *Immunity* (2002) 17(5):583–91. doi: 10.1016/S1074-7613(02)00446-6
26. Piao W, Song C, Chen H, Wahl LM, Fitzgerald KA, O'Neill LA, et al. Tyrosine Phosphorylation of MyD88 Adapter-Like (Mal) is Critical for Signal Transduction and Blocked in Endotoxin Tolerance. *J Biol Chem* (2008) 283(6):3109–19. doi: 10.1074/jbc.M707400200
27. Paracha RZ, Ali A, Ahmad J, Hussain R, Niazi U, Muhammad SA. Structural Evaluation of BTK and PKCdelta Mediated Phosphorylation of MAL at Positions Tyr86 and Tyr106. *Comput Biol Chem* (2014) 51:22–35. doi: 10.1016/j.compbiolchem.2014.04.001
28. Jefferies CA, O'Neill LA. Bruton's Tyrosine Kinase (Btk)-The Critical Tyrosine Kinase in LPS Signalling? *Immunol Lett* (2004) 92(1-2):15–22. doi: 10.1016/j.imlet.2003.11.017
29. Kubo-Murai M, Hazeki K, Sukenobu N, Yoshikawa K, Nigorikawa K, Inoue K, et al. Protein Kinase Cdelta Binds TIRAP/Mal to Participate in TLR Signaling. *Mol Immunol* (2007) 44(9):2257–64. doi: 10.1016/j.molimm.2006.11.005
30. Baig MS, Liu D, Muthu K, Roy A, Saqib U, Naim A, et al. Heterotrimeric Complex of P38 MAPK, PKCdelta, and TIRAP is Required for AP1 Mediated Inflammatory Response. *Int Immunopharmacol* (2017) 48:211–8. doi: 10.1016/j.intimp.2017.04.028
31. Yang Y, Kim SC, Yu T, Yi YS, Rhee MH, Sung GH, et al. Functional Roles of P38 Mitogen-Activated Protein Kinase in Macrophage-Mediated Inflammatory Responses. *Mediators Inflammation* (2014) 2014:352371. doi: 10.1155/2014/352371
32. Srivastava M, Saqib U, Banerjee S, Wary K, Kizil B, Muthu K, et al. Inhibition of the TIRAP-C-Jun Interaction as a Therapeutic Strategy for AP1-Mediated

Inflammatory Responses. *Int Immunopharmacol* (2019) 71:188–97. doi: 10.1016/j.intimp.2019.03.031
33. Miggin SM, Pålsson-McDermott E, Dunne A, Jefferies C, Pinteaux E, Banahan K, et al. NF-κb Activation by the Toll-IL-1 Receptor Domain Protein MyD88 Adapter-Like is Regulated by Caspase-1. *Proc Natl Acad Sci USA* (2007) 104(9):3372–7. doi: 10.1073/pnas.0608100104
34. Ulrichts P, Bovijn C, Lievens S, Beyaert R, Tavernier J, Peelman F. Caspase-1 Targets the TLR Adaptor Mal at a Crucial TIR-Domain Interaction Site. *J Cell Sci* (2010) 123(Pt 2):256–65. doi: 10.1242/jcs.056002
35. Dunne A, Carpenter S, Brikos C, Gray P, Strelow A, Wesche H, et al. IRAK1 and IRAK4 Promote Phosphorylation, Ubiquitination, and Degradation of MyD88 Adaptor-Like (Mal). *J Biol Chem* (2016) 291(47):24802. doi: 10.1074/jbc.A109.098137
36. Halabi S, Sekine E, Verstak B, Gay NJ, Moncrieffe MC. Structure of the Toll/interleukin-1 Receptor (TIR) Domain of the B-Cell Adaptor That Links Phosphoinositide Metabolism With the Negative Regulation of the Toll-Like Receptor (TLR) Signalosome. *JJoBC* (2017) 292(2):652–60. doi: 10.1074/jbc.M116.761528
37. Ni M, MacFarlane AW, Toft M, Lowell CA, Campbell KS, Hamerman JA. B-Cell Adaptor for PI3K (BCAP) Negatively Regulates Toll-Like Receptor Signaling Through Activation of PI3K. *JPotNAoS* (2012) 109(1):267–72. doi: 10.1073/pnas.1111957108
38. Troutman TD, Hu W, Fulenchek S, Yamazaki T, Kurosaki T, Bazan JF, et al. Role for B-Cell Adapter for PI3K (BCAP) as a Signaling Adapter Linking Toll-Like Receptors (TLRs) to Serine/Threonine Kinases PI3K/Akt. *Proc Natl Acad Sci USA* (2012) 109(1):273–8. doi: 10.1073/pnas.1118579109
39. Lauenstein JU, Scherm MJ, Udgata A, Moncrieffe MC, Fisher DI, Gay NJ. Negative Regulation of TLR Signaling by BCAP Requires Dimerization of Its DBB Domain. *JTJoI* (2020) 204(8):2269–76. doi: 10.4049/jimmunol.1901210
40. Yamamoto M, Sato S, Hemmi H, Sanjo H, Uematsu S, Kaisho T, et al. Essential Role for TIRAP in Activation of the Signalling Cascade Shared by TLR2 and TLR4. *Nature* (2002) 420(6913):324–9. doi: 10.1038/nature01182
41. Sakaguchi M, Kinoshita R, Putranto EW, Ruma IMW, Sumardika IW, Youyi C, et al. Signal Diversity of Receptor for Advanced Glycation End Products. *Acta Med Okayama* (2017) 71(6):459–65. doi: 10.18926/AMO/55582
42. Chuang TH, Ulevitch RJ. Triad3A, an E3 Ubiquitin-Protein Ligase Regulating Toll-Like Receptors. *Nat Immunol* (2004) 5(5):495–502. doi: 10.1038/ni1066
43. Leifer CA, Medvedev AE. Molecular Mechanisms of Regulation of Toll-Like Receptor Signaling. *JJolb* (2016) 100(5):927–41. doi: 10.1189/jlb.2MR0316-117RR
44. Lannoy V, Côté-Biron A, Asselin C, Rivard NJCC. Signaling. Phosphatases in Toll-Like Receptors Signaling: The Unfairly-Forgotten. *Cell Commun Signal* (2021) 19(1):1–15. doi: 10.1186/s12964-020-00693-9
45. Chattopadhyay S, Sen GC. Tyrosine Phosphorylation in Toll-Like Receptor Signaling. *Cytokine Growth Factor Rev* (2014) 25(5):533–41. doi: 10.1016/j.cytogfr.2014.06.002
46. Jefferies CA, Doyle S, Brunner C, Dunne A, Brint E, Wietek C, et al. Bruton's Tyrosine Kinase Is a Toll/interleukin-1 Receptor Domain-Binding Protein That Participates in Nuclear Factor kappaB Activation by Toll-Like Receptor 4. *J Biol Chem* (2003) 278(28):26258–64. doi: 10.1074/jbc.M301484200
47. Steinberg SF. Distinctive Activation Mechanisms and Functions for Protein Kinase Cdelta. *Biochem J* (2004) 384(Pt 3):449–59. doi: 10.1042/BJ20040704
48. Gschwendt M, Kielbassa K, Kittstein W, Marks F. Tyrosine Phosphorylation and Stimulation of Protein Kinase C Delta From Porcine Spleen by Src In Vitro. Dependence on the Activated State of Protein Kinase C Delta. *FEBS Lett* (1994) 347(1):85–9. doi: 10.1016/0014-5793(94)00514-1
49. Rip J, De Bruijn MJ, Appelman MK, Pal Singh S, Hendriks RW, Corneth O. Toll-Like Receptor Signaling Drives Btk-Mediated Autoimmune Disease. *Front Immunol* (2019) 10:95. doi: 10.3389/fimmu.2019.00095
50. Chavakis T, Bierhaus A, Nawroth PP. RAGE (Receptor for Advanced Glycation End Products): A Central Player in the Inflammatory Response. *Microbes Infect* (2004) 6(13):1219–25. doi: 10.1016/j.micinf.2004.08.004
51. Hudson BI, Lippman ME. Targeting RAGE Signaling in Inflammatory Disease. *Annu Rev Med* (2018) 69:349–64. doi: 10.1146/annurev-med-041316-085215
52. Sparvero LJ, Asafu-Adjei D, Kang R, Tang D, Amin N, Im J, et al. RAGE (Receptor for Advanced Glycation Endproducts), RAGE ligandsAnd Their Role in Cancer and Inflammation. *J Transl Med* (2009) 7:17. doi: 10.1186/1479-5876-7-17
53. Bierhaus A, Humpert PM, Morcos M, Wendt T, Chavakis T, Arnold B, et al. Understanding RAGE, The Receptor for Advanced Glycation End Products. *J Mol Med (Berl)* (2005) 83(11):876–86. doi: 10.1007/s00109-005-0688-7
54. Kierdorf K, Fritz G. RAGE Regulation and Signaling in Inflammation and Beyond. *J Leukoc Biol* (2013) 94(1):55–68. doi: 10.1189/jlb.1012519
55. Prantner D, Nallar S, Vogel SNJTFJ. The Role of RAGE in Host Pathology and Crosstalk Between RAGE and TLR4 in Innate Immune Signal Transduction Pathways. *FASEB J* (2020) 34(12):15659–74. doi: 10.1096/fj.202002136R
56. Watanabe M, Toyomura T, Wake H, Liu K, Teshigawara K, Takahashi H, et al. Differential Contribution of Possible Pattern-Recognition Receptors to Advanced Glycation End Product–Induced Cellular Responses in Macrophage-Like Raw264. 7 cells. *Biotechnol Appl Biochem* (2020) 67:(2):265–72. doi: 10.1002/bab.1843
57. Putranto EW, Murata H, Yamamoto KI, Kataoka K, Yamada H, Futami JI, et al. Inhibition of RAGE Signaling Through the Intracellular Delivery of Inhibitor Peptides by PEI Cationization. *Int J Mol Med* (2013) 32(4):938–44. doi: 10.3892/ijmm.2013.1467
58. Ishii KJ, Koyama S, Nakagawa A, Coban C, Akira S. Host Innate Immune Receptors and Beyond: Making Sense of Microbial Infections. *Cell Host Microbe* (2008) 3(6):352–63. doi: 10.1016/j.chom.2008.05.003
59. Jin MS, Kim SE, Heo JY, Lee ME, Kim HM, Paik SG, et al. Crystal Structure of the TLR1-TLR2 Heterodimer Induced by Binding of a Tri-Acylated Lipopeptide. *Cell* (2007) 130(6):1071–82. doi: 10.1016/j.cell.2007.09.008
60. Henneke P, Dramsi S, Mancuso G, Chraibi K, Pellegrini E, Theilacker C, et al. Lipoproteins are Critical TLR2 Activating Toxins in Group B Streptococcal Sepsis. *J Immunol* (2008) 180(9):6149–58. doi: 10.4049/jimmunol.180.9.6149
61. Parihar SP, Ozturk M, Marakalala MJ, Loots DT, Hurdayal R, Beukes D, et al. Protein Kinase C-Delta (PKCdelta), a Marker of Inflammation and Tuberculosis Disease Progression in Humans, is Important for Optimal Macrophage Killing Effector Functions and Survival in Mice. *Mucosal Immunol* (2018) 11(2):579–80. doi: 10.1038/mi.2017.108
62. Dixit R, Barnett B, Lazarus JE, Tokito M, Goldman YE, Holzbaur EL. Microtubule Plus-End Tracking by CLIP-170 Requires Eb1. *Proc Natl Acad Sci USA* (2009) 106(2):492–7. doi: 10.1073/pnas.0807614106
63. Maekawa H, Schiebel E. CLIP-170 Family Members: A Motor-Driven Ride to Microtubule Plus Ends. *Dev Cell* (2004) 6(6):746–8. doi: 10.1016/j.devcel.2004.05.017
64. Pierre P, Scheel J, Rickard JE, Kreis TE. CLIP-170 Links Endocytic Vesicles to Microtubules. *Cell* (1992) 70(6):887–900. doi: 10.1016/0092-8674(92)90240-D
65. Sengupta D, Koblansky A, Gaines J, Brown T, West AP, Zhang D, et al. Subversion of Innate Immune Responses by Brucella Through the Targeted Degradation of the TLR Signaling Adapter, MAL. *J Immunol* (2010) 184(2):956–64. doi: 10.4049/jimmunol.0902008
66. Murugan S, Jakka P, Namani S, Mujumdar V, Radhakrishnan G. The Neurosteroid Pregnenolone Promotes Degradation of Key Proteins in the Innate Immune Signaling to Suppress Inflammation. *J Biol Chem* (2019) 294(12):4596–607. doi: 10.1074/jbc.RA118.005543
67. Atsaves V, Leventaki V, Rassidakis GZ, Claret FXJC. AP-1 Transcription Factors as Regulators of Immune Responses in Cancer. *Cancers (Basel)* (2019) 11(7):1037. doi: 10.3390/cancers11071037
68. Eferl R, Wagner EF. AP-1: A Double-Edged Sword in Tumorigenesis. *Nat Rev Cancer* (2003) 3(11):859–68. doi: 10.1038/nrc1209
69. Kerppola TK, Curran T. Fos-Jun Heterodimers and Jun Homodimers Bend DNA in Opposite Orientations: Implications for Transcription Factor Cooperativity. *Cell* (1991) 66(2):317–26. doi: 10.1016/0092-8674(91)90621-5
70. Wisdom R. AP-1: One Switch for Many Signals. *Exp Cell Res* (1999) 253(1):180–5. doi: 10.1006/excr.1999.4685
71. Chida K, Nagamori S, Kuroki T. Nuclear Translocation of Fos is Stimulated by Interaction With Jun Through the Leucine Zipper. *Cell Mol Life Sci* (1999) 55(2):297–302. doi: 10.1007/s000180050291
72. Liu W, Ouyang X, Yang J, Liu J, Li Q, Gu Y, et al. AP-1 Activated by Toll-Like Receptors Regulates Expression of IL-23 P19. *J Biol Chem* (2009) 284(36):24006–16. doi: 10.1074/jbc.M109.025528
73. Liu X, Yin S, Chen Y, Wu Y, Zheng W, Dong H, et al. LPSinduced Proinflammatory Cytokine Expression in Human Airway Epithelial Cells

and Macrophages *via* NFkappaB, STAT3 or AP1 Activation. *Mol Med Rep* (2018) 17(4):5484–91. doi: 10.3892/mmr.2018.8542
74. Srivastava M, Baig MS. NOS1 Mediates AP1 Nuclear Translocation and Inflammatory Response. *BioMed Pharmacother* (2018) 102:839–47. doi: 10.1016/j.biopha.2018.03.069
75. Schonthaler HB, Guinea-Viniegra J, Wagner EF. Targeting Inflammation by Modulating the Jun/AP-1 Pathway. *Ann Rheum Dis* (2011) 70 Suppl 1:i109–12. doi: 10.1136/ard.2010.140533
76. Abraham C, Vogel SN, Perkins DJ. Signaling Mechanisms Regulating Innate Immune Responses. In: *Mucosal Immunology*. Cambridge, Massachusetts, United States: Academic Press (2015). p. 605–22. Academic Press
77. Boatright KM, Renatus M, Scott FL, Sperandio S, Shin H, Pedersen IM, et al. A Unified Model for Apical Caspase Activation. *Mol Cell* (2003) 11(2):529–41. doi: 10.1016/S1097-2765(03)00051-0
78. Lamkanfi M, Kalai M, Saelens X, Declercq W, Vandenabeele P. Caspase-1 Activates Nuclear Factor of the Kappa-Enhancer in B Cells Independently of its Enzymatic Activity. *J Biol Chem* (2004) 279(23):24785–93. doi: 10.1074/jbc.M400985200
79. Broz P, von Moltke J, Jones JW, Vance RE, Monack DM. Differential Requirement for Caspase-1 Autoproteolysis in Pathogen-Induced Cell Death and Cytokine Processing. *Cell Host Microbe* (2010) 8(6):471–83. doi: 10.1016/j.chom.2010.11.007
80. Martinon F, Mayor A, Tschopp J. The Inflammasomes: Guardians of the Body. *Annu Rev Immunol* (2009) 27:229–65. doi: 10.1146/annurev.immunol.021908.132715
81. Thornberry NA, Bull HG, Calaycay JR, Chapman KT, Howard AD, Kostura MJ, et al. A Novel Heterodimeric Cysteine Protease Is Required for Interleukin-1βprocessing in Monocytes. *Nature* (1992) 356(6372):768–74. doi: 10.1038/356768a0
82. Xie P. TRAF Molecules in Cell Signaling and in Human Diseases. *J Mol Signal* (2013) 8(1):7. doi: 10.1186/1750-2187-8-7
83. Li X, Zhong C-Q, Yin Z, Qi H, Xu F, He Q, et al. Data-Driven Modeling Identifies TIRAP-Independent MyD88 Activation Complex and Myddosome Assembly Strategy in LPS/TLR4 Signaling. *Int J Mol Sci* (2020) 21(9):3061. doi: 10.3390/ijms21093061
84. Janssens S, Beyaert R. Functional Diversity and Regulation of Different Interleukin-1 Receptor-Associated Kinase (IRAK) Family Members. *Mol Cell* (2003) 11(2):293–302. doi: 10.1016/S1097-2765(03)00053-4
85. Flo TH, Aderem A. Pathogen Recognition by Toll-Like Receptors. In: L Bertók, DA Chow, editors. *NeuroImmune Biology*, vol. 5p . Amsterdam, Netherlands: Elsevier (2005). p. 167–82. Elsevier
86. de Diego RP, Rodríguez-Gallego C. Chapter 34 - Other TLR Pathway Defects. In: KE Sullivan, ER Stiehm, editors. *Stiehm's Immune Deficiencies*. Amsterdam: Academic Press (2014). p. 687–710.
87. Kumar H, Takeuchi O, Akira S. Toll-Like Receptors. In: WJ Lennarz, MD Lane, editors. *Encyclopedia of Biological Chemistry*, *2nd ed.* Waltham: Academic Press (2013). p. 396–401.
88. Mandraju R, Troutman TD, Pasare C. Toll-Like Receptor Function and Signaling. In: *Reference Module in Biomedical Sciences*. Amsterdam, Netherlands: Elsevier (2014).
89. Biswas C. Chapter 18 - Inflammation in Systemic Immune Diseases: Role of TLR9 Signaling and the Resultant Oxidative Stress in Pathology of Lupus. In: S Chatterjee, W Jungraithmayr, D Bagchi, editors. *Immunity and Inflammation in Health and Disease*. Cambridge, Massachusetts, United States: Academic Press (2018). p. 223–37.
90. Yoshimura A, Naka T, Kubo M. SOCS Proteins, Cytokine Signalling and Immune Regulation. *Nat Rev Immunol* (2007) 7(6):454–65. doi: 10.1038/nri2093
91. Sharma J, Larkin J3rd. Therapeutic Implication of SOCS1 Modulation in the Treatment of Autoimmunity and Cancer. *Front Pharmacol* (2019) 10:324. doi: 10.3389/fphar.2019.00324
92. Baig MS, Zaichick SV, Mao M, de Abreu AL, Bakhshi FR, Hart PC, et al. NOS1-Derived Nitric Oxide Promotes NF-kappaB Transcriptional Activity Through Inhibition of Suppressor of Cytokine Signaling-1. *J Exp Med* (2015) 212(10):1725–38. doi: 10.1084/jem.20140654
93. Medvedev AE, Piao W, Shoenfelt J, Rhee SH, Chen H, Basu S, et al. Role of TLR4 Tyrosine Phosphorylation in Signal Transduction and Endotoxin Tolerance. *J Biol Chem* (2007) 282(22):16042–53. doi: 10.1074/jbc.M606781200
94. Zhao X, Xiong W, Xiao S, Tang TX, Ellena JF, Armstrong GS, et al. Membrane Targeting of TIRAP is Negatively Regulated by Phosphorylation in its Phosphoinositide-Binding Motif. *Sci Rep* (2017) 7:43043. doi: 10.1038/srep43043
95. Hughes MM, Lavrencic P, Coll RC, Ve T, Ryan DG, Williams NC, et al. Solution Structure of the TLR Adaptor MAL/TIRAP Reveals an Intact BB Loop and Supports MAL Cys91 Glutathionylation for Signaling. *Proc Natl Acad Sci USA* (2017) 114(32):E6480–E9. doi: 10.1073/pnas.1701868114
96. Xue Y, Liu Z, Cao J, Ma Q, Gao X, Wang Q, et al. GPS 2.1: Enhanced Prediction of Kinase-Specific Phosphorylation Sites With an Algorithm of Motif Length Selection. *Protein Eng Des Sel* (2011) 24(3):255–60. doi: 10.1093/protein/gzq094
97. Blom N, Sicheritz-Pontén T, Gupta R, Gammeltoft S, Brunak SJP. Prediction of Post-Translational Glycosylation and Phosphorylation of Proteins From the Amino Acid Sequence. *Proteomics* (2004) 4(6):1633–49. doi: 10.1002/pmic.200300771
98. Xue Y, Liu Z, Gao X, Jin C, Wen L, Yao X, et al. GPS-SNO: Computational Prediction of Protein S-Nitrosylation Sites With a Modified GPS Algorithm. *PloS One* (2010) 5(6):e11290. doi: 10.1371/journal.pone.0011290
99. Xie Y, Luo X, Li Y, Chen L, Ma W, Huang J, et al. DeepNitro: Prediction of Protein Nitration and Nitrosylation Sites by Deep Learning. *Genomics Proteomics Bioinformatics* (2018) 16(4):294–306. doi: 10.1016/j.gpb.2018.04.007
100. Lee T-Y, Chen Y-J, Lu T-C, Huang H-D, Chen Y-J. SNOSite: Exploiting Maximal Dependence Decomposition to Identify Cysteine S-Nitrosylation With Substrate Site Specificity. *PLoS One* (2011) 6(7):e21849. doi: 10.1371/journal.pone.0021849
101. Fulgione A, Papaianni M, Cuomo P, Paris D, Romano M, Tuccillo C, et al. Interaction Between MyD88, TIRAP and IL1RL1 Against Helicobacter Pylori Infection. *Sci Rep* (2020) 10(1):1–13. doi: 10.1038/s41598-020-72974-9

Conflict of Interest: The authors declare that the research was conducted in the absence of any commercial or financial relationships that could be construed as a potential conflict of interest.

NOS1-derived nitric oxide promotes NF-κB transcriptional activity through inhibition of suppressor of cytokine signaling-1

Mirza Saqib Baig,[1,2]* Sofia V. Zaichick,[1,2]* Mao Mao,[1,2]* Andre L. de Abreu,[1,2,7] Farnaz R. Bakhshi,[2] Peter C. Hart,[1,6] Uzma Saqib,[2] Jing Deng,[1] Saurabh Chatterjee,[3] Michelle L. Block,[4] Stephen M. Vogel,[2] Asrar B. Malik,[2] Marcia E.L. Consolaro,[7] John W. Christman,[1] Richard D. Minshall,[2,5] Benjamin N. Gantner,[2] and Marcelo G. Bonini[1,2,6]

[1]Department of Medicine, [2]Department of Pharmacology, [3]Department of Anesthesiology, and [4]Department of Pathology, University of Illinois College of Medicine, Chicago, IL 60607
[5]Department of Environmental Health Sciences, University of South Carolina, Columbia, SC 29208
[6]Department of Anatomy and Cell Biology, Stark Neurosciences Research Institute, Indiana University, Indianapolis, IN 46202
[7]Programa de Biociencias Aplicadas a Farmacia (PBF), Universidade Estadual de Maringa, Maringa 87020-900, Brazil

The NF-κB pathway is central to the regulation of inflammation. Here, we demonstrate that the low-output nitric oxide (NO) synthase 1 (NOS1 or nNOS) plays a critical role in the inflammatory response by promoting the activity of NF-κB. Specifically, NOS1-derived NO production in macrophages leads to proteolysis of suppressor of cytokine signaling 1 (SOCS1), alleviating its repression of NF-κB transcriptional activity. As a result, *NOS1*$^{-/-}$ mice demonstrate reduced cytokine production, lung injury, and mortality when subjected to two different models of sepsis. Isolated *NOS1*$^{-/-}$ macrophages demonstrate similar defects in proinflammatory transcription on challenge with Gram-negative bacterial LPS. Consistently, we found that activated *NOS1*$^{-/-}$ macrophages contain increased SOCS1 protein and decreased levels of p65 protein compared with wild-type cells. NOS1-dependent S-nitrosation of SOCS1 impairs its binding to p65 and targets SOCS1 for proteolysis. Treatment of *NOS1*$^{-/-}$ cells with exogenous NO rescues both SOCS1 degradation and stabilization of p65 protein. Point mutation analysis demonstrated that both Cys147 and Cys179 on SOCS1 are required for its NO-dependent degradation. These findings demonstrate a fundamental role for NOS1-derived NO in regulating TLR4-mediated inflammatory gene transcription, as well as the intensity and duration of the resulting host immune response.

CORRESPONDENCE
Marcelo G. Bonini:
mbonini@uic.edu
OR
Benjamin N. Gantner:
bgantner@uic.edu

Abbreviations used: BMDM, BM-derived macrophage; CLP, cecal ligation and puncture; ELAM, endothelial cell-leukocyte adhesion molecule; GAPDH, glyceraldehyde 3-phosphate dehydrogenase; GSNO, S-nitrosoglutathione; HDAC, histone deacetylase; NO, nitric oxide; NOS, NO synthase; SOCS, suppressor of cytokine signaling; TRIM, 1-(2-Trifluoromethylphenyl) imidazole.

Orchestration of the severity, duration, and location of inflammation is critical to achieving sterilizing immunity while minimizing tissue injury. The NF-κB pathway is central to establishing this balance. NF-κB promotes transcription of genes involved in every aspect of the immune response, from differentiation and homeostatic regulation of immune cells, to modulation of barrier function and leukocyte recruitment during acute activation and the deployment of immune effector mechanisms that mediate antimicrobial activity (Xia et al., 1997; Badrichani et al., 1999; Jeon et al., 1999; Alcamo et al., 2001; Tiruppathi et al., 2008; Jacobson and Birukov, 2009; Lawrence, 2009; Baltimore, 2011; Li et al., 2011; Pittet et al., 2011; Ruland, 2011; Sadik et al., 2011; Fieren, 2012; Koelink et al., 2012; Summers deLuca and Gommerman, 2012; Sun and Karin, 2012; Takizawa et al., 2012). Disrupted NF-κB signaling leads to defective pathogen clearance, autoimmunity, and tissue injury (Bowie and O'Neill, 2000; Javaid et al., 2003; Aktan, 2004; Dixon, 2004; Block and Hong, 2005; Parsons et al., 2005; Dombrovskiy et al., 2007; Panettieri et al., 2008; Jacobson and Birukov, 2009; Liu, 2011; Nacher and Hidalgo,

*M.S. Baig, S.V. Zaichick, and M. Mao contributed equally to this paper.

The Rockefeller University Press $30.00
J. Exp. Med. 2015 Vol. 212 No. 10 1725–1738
www.jem.org/cgi/doi/10.1084/jem.20140654

2011; Rossi et al., 2011; Ruland, 2011; Edgley et al., 2012; Ma and Malynn, 2012).

NF-κB signaling is complex, leading to multiple distinct transcription complexes whose formation and stability are known to be regulated by a wide array of protein modifications, including phosphorylation, ubiquitination, and glutathiolation, as well as modifications by reactive oxygen and nitrogen species (Bowie and O'Neill, 2000; Marshall and Stamler, 2001; Ben-Neriah, 2003; Bubici et al., 2006; Mattioli et al., 2006; Nicholas et al., 2007; Geng et al., 2009; Lin et al., 2012; Sabatel et al., 2012). Nitric oxide (NO) has long been appreciated to promote feedback inhibition of NF-κB because of the important role of the high output NO synthase 2 (NOS) in inflammation. However, mammals encode three distinct NOS isozymes: neuronal (nNOS or NOS1), inducible (iNOS or NOS2), and endothelial (eNOS or NOS3; Knowles and Moncada, 1994). To determine the precise roles for each of these in inflammatory signaling, we analyzed animals with targeted mutations in each of the three NOS isoforms in two models of sepsis. We demonstrate that, unique among the three NOS enzymes, NO produced by the low-output NOS1 plays a critical role in promoting NF-κB–mediated proinflammatory cytokine transcription in animals and in isolated macrophages.

The canonical NF-κB complex is comprised of p65 and p50 subunits held inactive in the cytoplasm by IκB. The targeted proteolysis of IκB results in nuclear translocation of the p65:p50 complex, and subsequent transcriptional activation. IκB degradation is promoted by a large number of proinflammatory signaling pathways, and its preservation is the target of many antiinflammatory pathways. (Jacobs and Harrison, 1998; Vanden Berghe et al., 1999; Basak et al., 2007; Baltimore, 2011; Ruland, 2011). We therefore determined its status in the *NOS1*$^{-/-}$ macrophages challenged with LPS, but found no defect in IκB degradation. Instead, we found that p65 protein levels were not maintained in the knockout cells. Suppressor of cytokine signaling (SOCS1) has been reported to promote the degradation of DNA-bound p65 protein leading to the suppression of NF-κB activity and inflammation (Kinjyo et al., 2002; Nakagawa et al., 2002; Ben-Neriah, 2003; Park et al., 2003; Ryo et al., 2003; Baetz et al., 2004; Gingras et al., 2004; Strebovsky et al., 2011; Linossi and Nicholson, 2012). We show that NOS1-derived NO promotes the S-nitrosation of SOCS1, and that this ablates its capacity to bind and target p65 for degradation. Therefore, we show that NO from NOS1 permits the full transcriptional activation of NF-κB in macrophages by suppressing SOCS1.

RESULTS

NOS1$^{-/-}$ animals are protected from model septic injury and mortality, whereas *NOS2*$^{-/-}$ and *NOS3*$^{-/-}$ animals demonstrate greater susceptibility

We analyzed the response of *NOS1*$^{-/-}$, *NOS2*$^{-/-}$, and *NOS3*$^{-/-}$ animals with an experimental model of sepsis: i.p. LPS injection. Similar to earlier studies, we observed increased mortality in *NOS2*$^{-/-}$ and *NOS3*$^{-/-}$ animals (Hickey et al., 1997; Wang et al., 2004; Miki et al., 2005; Fig. 1 A). In contrast, *NOS1*$^{-/-}$ mice showed increased survival when compared with control animals (Fig. 1 A). We tested whether compensatory expression changes in NOS1 could help to explain the susceptible *NOS2*$^{-/-}$ or *NOS3*$^{-/-}$ phenotypes, but we detected comparable levels of NOS1 expression in WT, *NOS2*$^{-/-}$, and *NOS3*$^{-/-}$ (unpublished data). We also tested responses to a polymicrobial sepsis model, cecal ligation and puncture (CLP). Again, *NOS1*$^{-/-}$ animals were protected compared with WT (Fig. 1 B). Acute lung injury is a major cause of morbidity and mortality associated with acute systemic inflammation (Matthay and Zemans, 2011). Although WT and *NOS3*$^{-/-}$ lungs demonstrated marked inflammatory remodeling, as well as increased vascular permeability assessed by capillary filtration analysis (K_{fc}), *NOS1*$^{-/-}$ lungs were protected in both assays (Fig. 1, C and D). To determine if these effects were caused by the loss of NOS1 and not by any compensatory effects of gene deletion, we also treated WT mice with the NOS1/NOS2 inhibitor 1-(2-Trifluoromethylphenyl) imidazole, TRIM (Handy et al., 1995). In agreement with many previous studies, we find that NOS2 is not significantly expressed until hours after the activation of inflammation, and expect that TRIM's mechanism of action at this time should be solely through NOS1 (see also Fig. 5, F and G). Consistent with this, TRIM treatment recapitulated the results of genetic ablation of NOS1 for both mortality and histological correlates of injury (Fig. 1, E and F). Although NOS2 and NOS3 play protective roles in septic injury, we demonstrate that NOS1, uniquely, promotes the injury associated with model sepsis.

NOS1 is required for TLR4-mediated cytokine production and NF-κB activation, in vitro and in vivo

De novo transcription and translation of cytokines plays a critical role in promoting inflammatory tissue injury during sepsis. In accordance with their protection from septic injury, we observed that *NOS1*$^{-/-}$ mice displayed significantly decreased plasma cytokine responses 8 h after i.p. LPS treatment compared with WT, whereas *NOS2*$^{-/-}$ and *NOS3*$^{-/-}$ mice mounted normal cytokine responses (Fig. 2 A). Macrophages are critical cellular mediators of inflammation in vivo (MacMicking, et al., 1997). We analyzed NOS1 function in these cells and found that they recapitulated the in vivo phenotype of NOS1 deficiency. BM-derived macrophages (BMDMs) prepared from *NOS1*$^{-/-}$ mice demonstrated significant reductions in mRNA and protein accumulation for an array of cytokines (TNF, IL1β, IL6, and MIP2; Fig. 2, B–D). Acute inhibition of NOS1 in WT BMDM by pretreatment with TRIM also reduced cytokine transcriptional responses to LPS treatment (Fig. 2 C). These broad defects in proinflammatory cytokine transcription led us to investigate the signaling and transcriptional pathways downstream of TLR4. NF-κB activation is critical for expression of a wide variety of inflammatory cytokines, so we interrogated this pathway in the *NOS1*$^{-/-}$ cells. Early signaling events in the pathway converge on the degradation of IκB, which liberates the transcription factor complex to the nucleus. *NOS1*$^{-/-}$ BMDMs responded to LPS treatment by degrading IκB similarly to WT cells, suggesting that the earliest signaling events

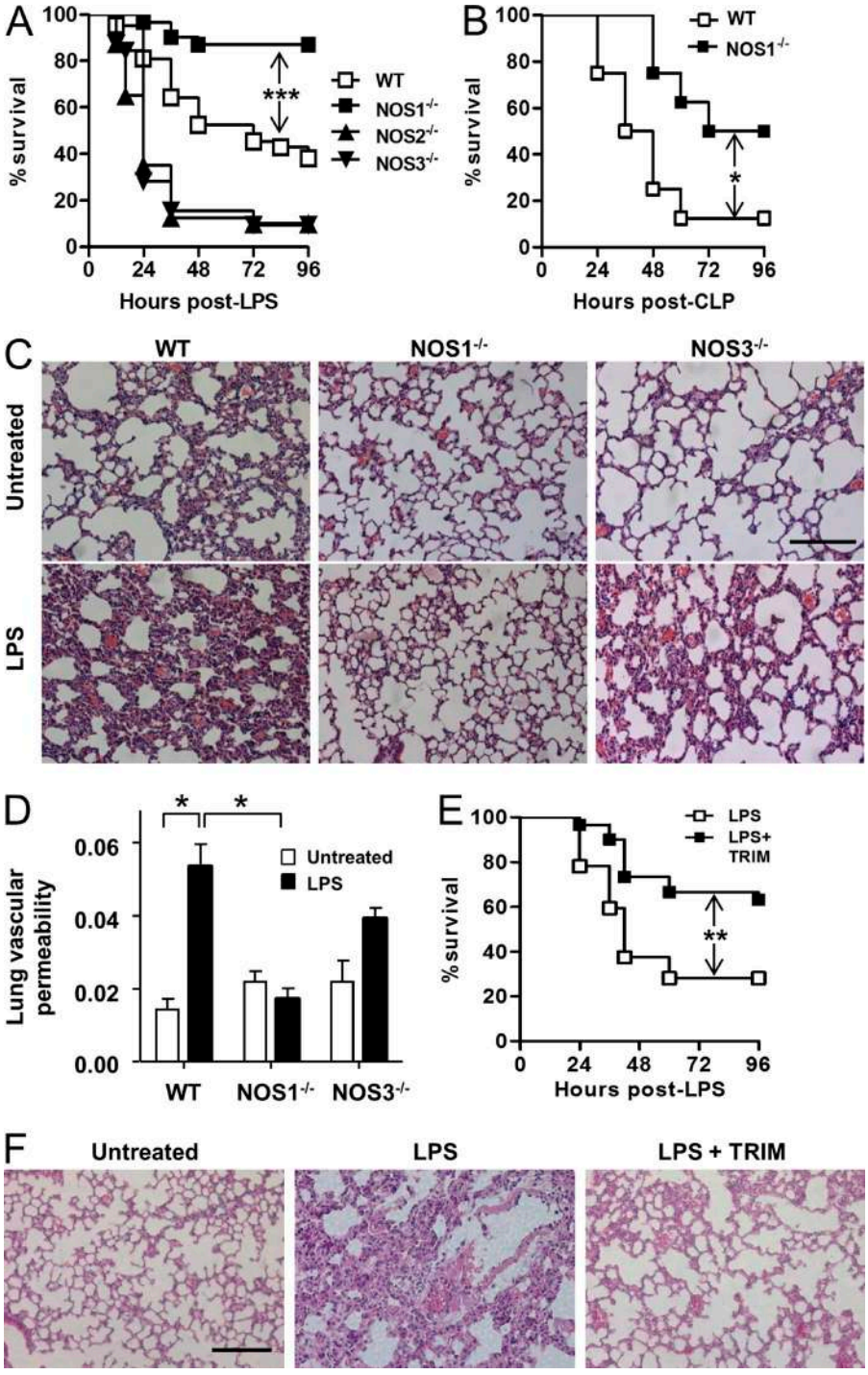

Figure 1. NOS1 deficiency protects against model septic injury. (A) Survival of WT ($n = 42$), *NOS1*$^{-/-}$ ($n = 31$), *NOS2*$^{-/-}$ ($n = 40$), and *NOS3*$^{-/-}$ ($n = 32$) mice injected with LPS (30 mg/kg, i.p.), compiled from at least 3 independent experiments using 10 mice per group, or (B) WT ($n = 8$) and *NOS1*$^{-/-}$ ($n = 8$) mice, compiled from 2 independent experiments, were subjected to CLP and survival was monitored for the indicated time. (C) Lungs of WT, *NOS3*$^{-/-}$, and *NOS1*$^{-/-}$ mice were harvested 8 h after i.p. LPS challenge and sections were stained with H&E. Representative images from three mice per phenotype analyzed in three independent experiments are shown. Bar, 100 µM. (D) Lung vascular permeability measurements (K_{fc}) of WT, *NOS3*$^{-/-}$, and *NOS1*$^{-/-}$, mice before and 8 h after LPS challenge. Three mice per phenotype were analyzed in three independent experiments. *, $P < 0.05$, Student's *t* test. (E) Survival of WT mice treated with LPS alone ($n = 32$) or pretreated for 2 h with TRIM (25 mg/kg, i.p.) before LPS ($n = 30$), compiled from at least 3 independent experiments with 10 mice per group (F). Lung histological analyses were performed on WT mice as in C, either control or with pretreatment with TRIM, as in E. Significance in A–C was determined using Fisher's exact test. *, $P < 0.02$ (B); **, $P < 0.001$ (E); ***, $P < 0.0005$ (A).

triggered by TLR4 are intact. Despite this, we found that re-expression of IκB after degradation is significantly diminished (Fig. 3, A and B). Because IκB is one of its major targets, we analyzed NF-κB transcriptional activation downstream of IκB degradation. Despite detecting an increase in nuclear p65 DNA-binding activity in LPS-treated WT BMDM, we saw no increase in *NOS1*$^{-/-}$ BMDM (Fig. 3 C). Consistent with this, a mouse macrophage cell line (RAW264.7) stably transfected with an NF-κB–driven luciferase reporter (endothelial cell–leukocyte adhesion molecule [ELAM] cells; Gantner et al., 2003) and treated with LPS for 6 h demonstrated significantly reduced luciferase reporter activity after pretreatment with TRIM (Fig. 3 D). Mice expressing another NF-κB–driven luciferase reporter ubiquitously as a transgene (HLL-mice) demonstrated that TRIM treatment could also significantly dampen systemic NF-κB activation in vivo, 24 h after LPS treatment (Sadikot et al., 2001; Fig. 3, E and F). Our findings demonstrate a novel and important role for NOS1 in promoting a broad array of

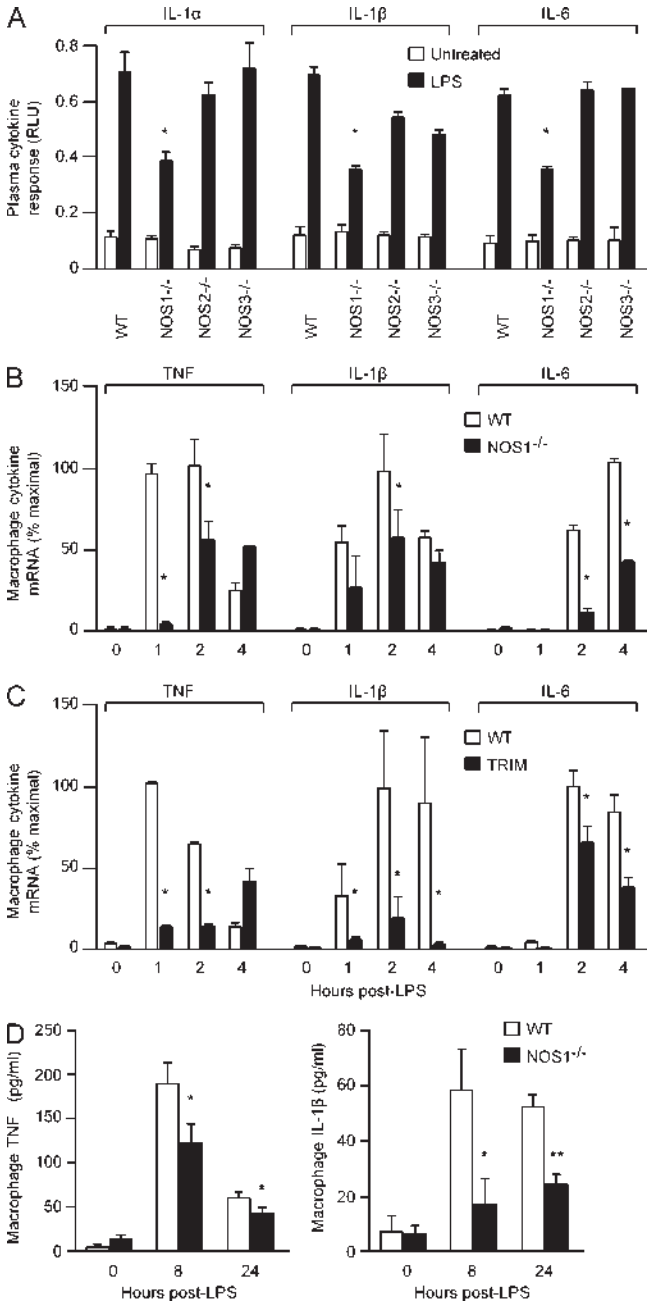

Figure 2. Proinflammatory cytokine responses to LPS are diminished in *NOS1*$^{-/-}$ animals and cultured macrophages. (A) IL-1α, IL-1β, and IL-6 in the plasma of WT, *NOS1*$^{-/-}$, *NOS2*$^{-/-}$, and *NOS3*$^{-/-}$ mice before and 8 h after LPS (30 mg/kg, i.p.) injection. Cytokine levels in plasma were assessed using a Luminex panel and expressed as relative light units (RLU). Nine mice for each treatment condition and genotype were analyzed and data are compiled from three independent experiments, mean ± SEM. *, P < 0.005 (Student's *t* test). (B) Quantitative RT-PCR analysis of cytokine mRNA expression of *TNF*, *IL-6*, and *IL-1*β in BMDMs isolated from WT and *NOS1*$^{-/-}$ mice and stimulated with LPS (250 ng/ml). *, P < 0.0005. (C) mRNA expression analysis of *TNF*, *IL-6*, and *IL-1*β in WT macrophages (no inhibitor) and WT macrophages treated 2 h with TRIM (100 nM) before LPS (250 ng/ml) stimulation. *, P < 0.003 (Student's *t* test). (D) ELISA measurements of TNF and IL-1β cytokine levels in culture media of LPS-activated BMDM (250 ng/ml). *, P < 0.02; **, P < 0.001 (Student's *t* test). Representative data are shown from three (B–D) independent experiments, and are expressed as mean ± SD.

proinflammatory cytokine expression by driving NF-κB DNA binding and transcriptional activation.

NOS1 is required to block proteolytic degradation of p65 in LPS-activated macrophages

Unexpectedly, *NOS1*$^{-/-}$ BMDM showed a rapid decrease in p65 protein levels after LPS stimulation, despite comparable expression of p65 in unstimulated cells. This was in clear contrast with WT or *NOS3*$^{-/-}$ cells, where p65 protein levels remained stable (Fig. 4, A and B). NF-κB p50, the canonical binding partner for p65, was not degraded in *NOS1*$^{-/-}$ or WT BMDM (Fig. 4 C and not depicted). p65 is central to canonical NF-κB transcription, so a reduction in its protein level could account for the cytokine transcriptional defects in the absence of NOS1 (Alcamo et al., 2001; Vallabhapurapu and Karin, 2009; Baltimore, 2011; Fig. 2). To determine whether the loss of p65 was caused by synthesis or degradation, we treated *NOS1*$^{-/-}$ macrophages with the proteasome inhibitor MG132, and were able to rescue p65 protein levels after LPS treatment (Fig. 4, A and B). Consistent with this, we compared p65 protein levels in *NOS1*$^{-/-}$ and WT BMDMs after blocking de novo protein synthesis with emetin (Grollman, 1968) and found that knockout cells still lost p65 protein after LPS treatment (Fig. 4, E and F). These results support the hypothesis that NOS1 blocks proteasomal degradation of p65 in macrophages, rather than affecting p65 synthesis. We prepared cytosolic and nuclear fractions from BMDMs and analyzed p65 protein abundance. Although little difference was detected in cytoplasmic p65, nuclear p65 protein was greatly depleted from *NOS1*$^{-/-}$ BMDMs (Fig. 4 D). This led us to determine the subcellular localization of NOS1 in macrophages. Using immunofluorescence imaging and nuclear fractionation of BMDMs, we found that NOS1 was mainly in the nucleus, regardless of the LPS-activation state of the cell (Fig. 5, A and B). This finding is consistent with other reports that NOS1 can function in the nucleus and further supports the hypothesis that this enzyme plays an important role in regulating gene expression (Yuan et al., 2004; Saluja et al., 2010; Villanueva and Giulivi, 2010). We then undertook functional characterization of NOS1 to ensure that it is enzymatically active in BMDMs. Consistent with previous observations that NOS1 is phosphorylated on Ser1412 on activation (Huang et al., 2012), we found that LPS treatment induced NOS1 phosphorylation on this site within minutes in BMDMs (Fig. 5 C). This correlated with two indirect measures of NO. We detected very early pulses of nitrite (60 min) and peroxynitrite (30 min) production in BMDMs. However, *NOS1*$^{-/-}$ BMDMs failed to produce either of these products of NO within this time frame (Fig. 5, D and E). Similarly, TRIM pretreatment blocked production of either product in WT cells (Fig. 5 E and not depicted). Consistent with NOS1 activity reported in other cell types, calcium ionophore

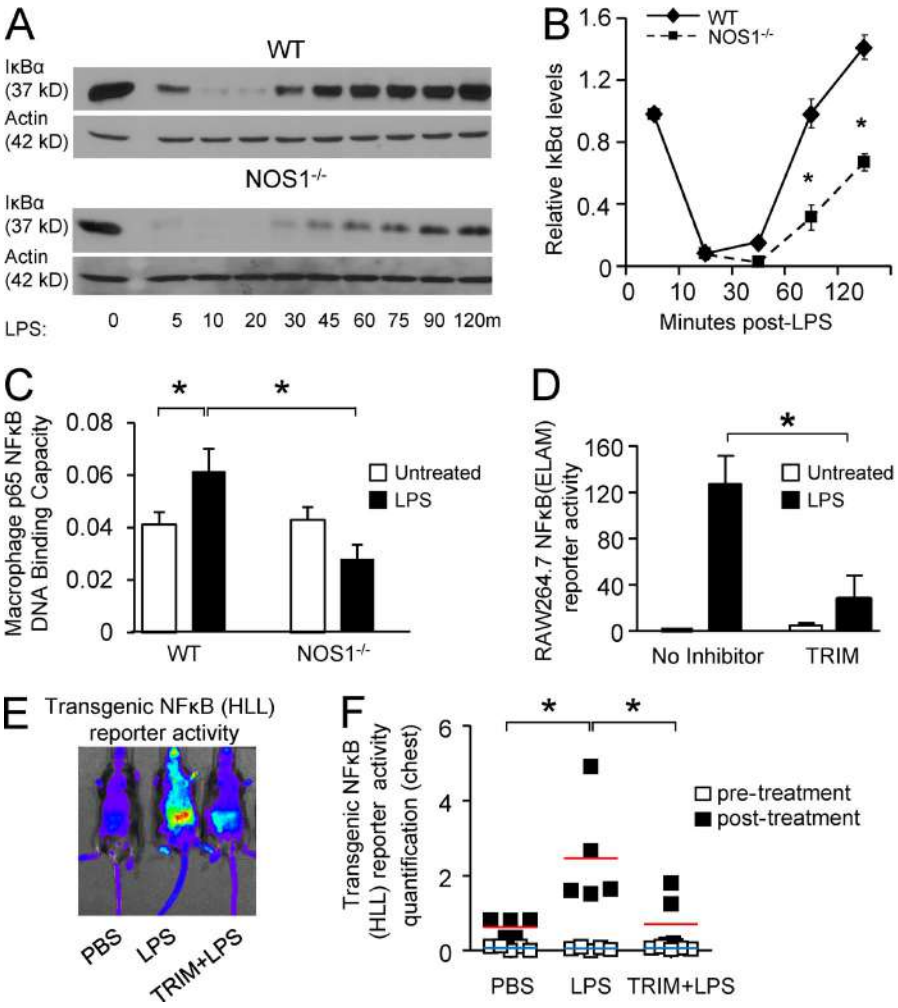

Figure 3. NOS1 is required for NF-κB transcriptional activation but not upstream signaling. (A) Representative immunoblots for IκB degradation after LPS treatment (250 ng/ml) from WT and *NOS1*$^{-/-}$ BMDMs. (B) Densitometry analysis of IκB levels as in (A), normalized to actin, presented as mean ± SEM of quantitation of three independent experiments. *, P < 0.02 (Student's *t* test). (C) p65 DNA-binding activity was assayed from the isolated nuclei of WT and *NOS1*$^{-/-}$ BMDM before and after LPS (250 ng/ml) for 1 h. *, P < 0.001, Student's *t* test. (D) RAW264.7 macrophage cell line stably expressing an NF-κB–driven luciferase reporter (ELAM) were pretreated with TRIM (50 µM) for 2 h and then stimulated with LPS (100 ng/ml) for 6 h. *, P < 0.0005, Student's *t* test. C and D are representative of three independent experiments, presented as mean ± SD of three replicates. Representative digital images of (E) and quantitation of (F) NF-κB transcriptional activity from mice expressing a transgenic luciferase reporter (HLL) 24 h after treatment with PBS (control), LPS or LPS after 2 h pretreatment with TRIM (50 mg/kg, i.p.) to inhibit NOS1. Luminescence was evaluated by IVIS 10 min after i.p. injection of 30 mg/kg luciferin. Quantitation focused on activity in the chest (*n* = 6 animals per group compiled from two separate experiments using 3 mice per treatment), and includes basal reporter activity before LPS or PBS treatment for comparison. *, P < 0.05 (Student's *t* test). Averages are shown as horizontal bars, red for treated, and blue for control values.

treatment drove nitrite production in WT, but not in *NOS1*$^{-/-}$ BMDMs (unpublished data). To exclude the possibility that NOS2 was contributing to early NO activity, we examined *NOS2* mRNA and protein at time points after LPS treatment. We found no detectable expression in WT or knockout cells until 4 h after LPS treatment, well after the early LPS-mediated NOS activity we detected (Fig. 5, F and G). Our data demonstrate that LPS stimulation activates mechanisms that promote p65 degradation, and that uniquely among the NOS family enzymes, NOS1 is capable of blocking this, and thereby, of maintaining p65 protein levels.

NOS1-derived NO mediates S-nitrosation of SOCS1, blocking its ability to target p65 for degradation

One mechanism reported to direct p65 protein degradation involves the antiinflammatory molecule SOCS1. SOCS1 is reported to mediate ubiquitination of DNA-bound p65 leading to its proteasomal lysis (Ben-Neriah, 2003; Ryo et al., 2003; Strebovsky et al., 2011). To determine if SOCS1 could be involved in NOS1-dependent signaling, we analyzed its protein expression in macrophages. WT, *NOS2*$^{-/-}$, and *NOS3*$^{-/-}$ BMDM demonstrate decreasing SOCS1 protein abundance for the time period examined. In contrast, *NOS1*$^{-/-}$ cells alone demonstrated accumulation of SOCS1 protein that tracked with the drop in p65 protein levels after LPS stimulation (Fig. 6 A). To determine if SOCS1 is a direct target of NO, we analyzed protein S-nitrosation. By performing biotin switch assays on MG132-treated cells (to retain protein that would otherwise be proteasomally degraded) we found that in WT BMDM, SOCS1 demonstrates low basal S-nitrosation that increases dramatically after 1-h LPS treatment. In stark contrast, *NOS1*$^{-/-}$ cells demonstrate much lower basal nitrosation and no detectable increase with LPS treatment (Fig. 6 B). *NOS2*$^{-/-}$ and *NOS3*$^{-/-}$ BMDM exhibited low basal and robust LPS-induced S-nitrosation, demonstrating that these enzymes are not required to modify SOCS1 during the time course we studied (Fig. 6 C). In addition to the effect on protein stability, we also found that NOS1 regulates the ability of SOCS1 to physically interact with p65. Immunoprecipitates of SOCS1 from MG132-treated BMDM show greater binding to p65 in *NOS1*$^{-/-}$ than in WT cells (Fig. 6 D). Finally, we tested the ability of exogenous NO to rescue the defects seen in the knockout macrophages

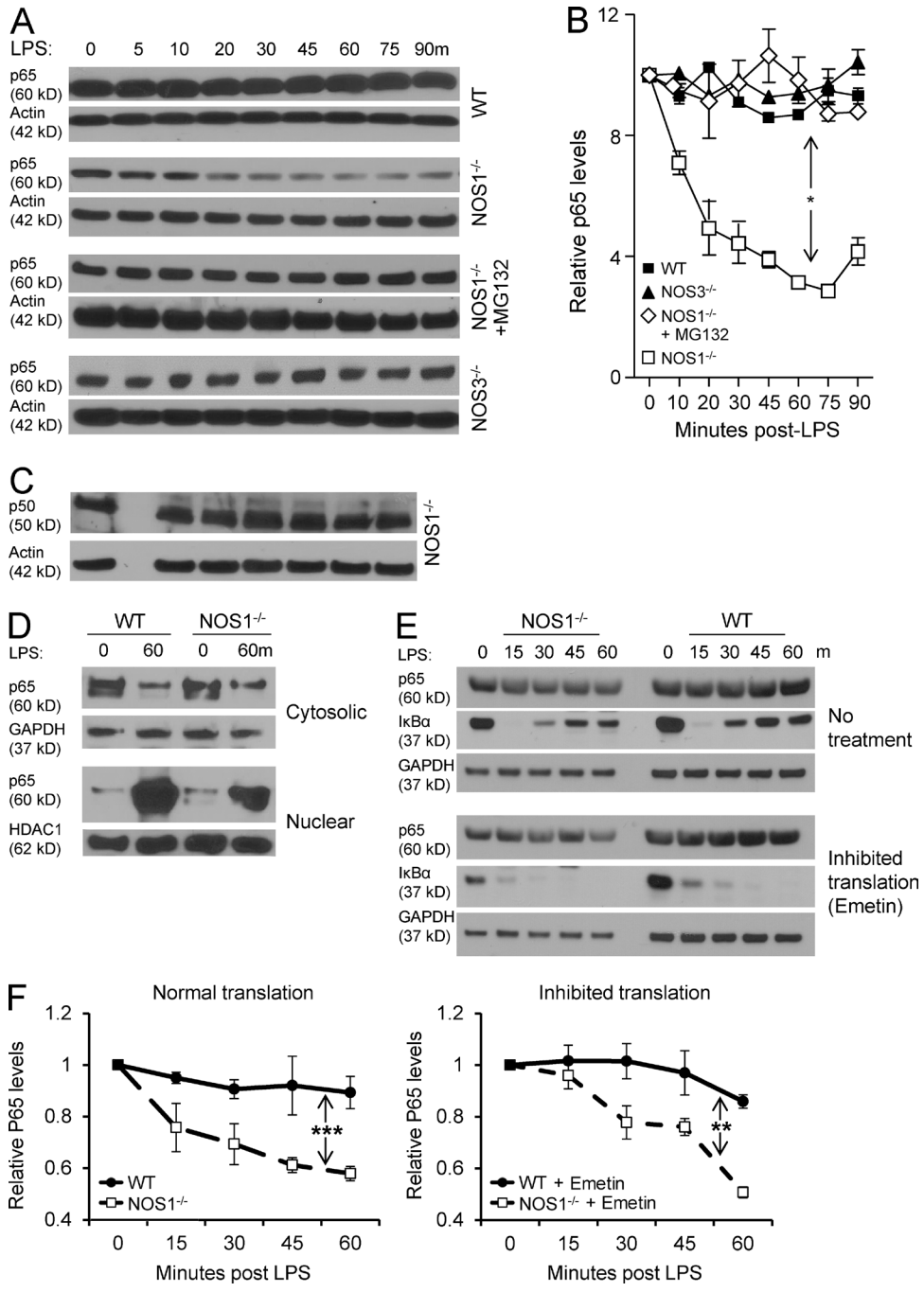

Figure 4. ***NOS1*$^{-/-}$ BMDM fail to maintain p65 protein levels after exposure to LPS.** Representative immunoblots (A) and densitometric quantitation (B) of NF-κB p65 protein levels in BMDM stimulated with LPS (250 ng/ml), normalized to actin, for the indicated times and genotypes. Where indicated, cells were pretreated with MG132 (50 µM, proteasome inhibitor). *, $P < 0.01$. (C) Immunoblot analysis of total NF-κB p50 levels in *NOS1*$^{-/-}$ macrophages after LPS (250 ng/ml). (D) Isolated cytoplasmic and nuclear fractions of WT and *NOS1*$^{-/-}$ BMDM were probed for p65 by immunoblot before and after LPS (250 ng/ml) for 60 min, GAPDH and HDAC1 are loading controls for cytoplasmic or nuclear protein, respectively. p65 protein degradation dynamics was assessed by (E) immunoblot and (F) densitometric quantitation (normalized to GAPDH) after inhibition of de novo protein synthesis by treatment of BMDM with emetin (100 µg/ml) or control, followed by LPS (250 ng/ml) for the indicated times. The loss of IκBα re-expression demonstrates the effective inhibition of protein translation. For all of the above experiments, representative blots are shown from 3 independent experiments and quantitation, based on all experiments, are presented as mean ± SEM. P-values were determined by Anova two-way test with Bonferroni post-test to compare replicates: *, $P < 0.02$; **, $P < 0.001$; and ***, $P < 0.0001$.

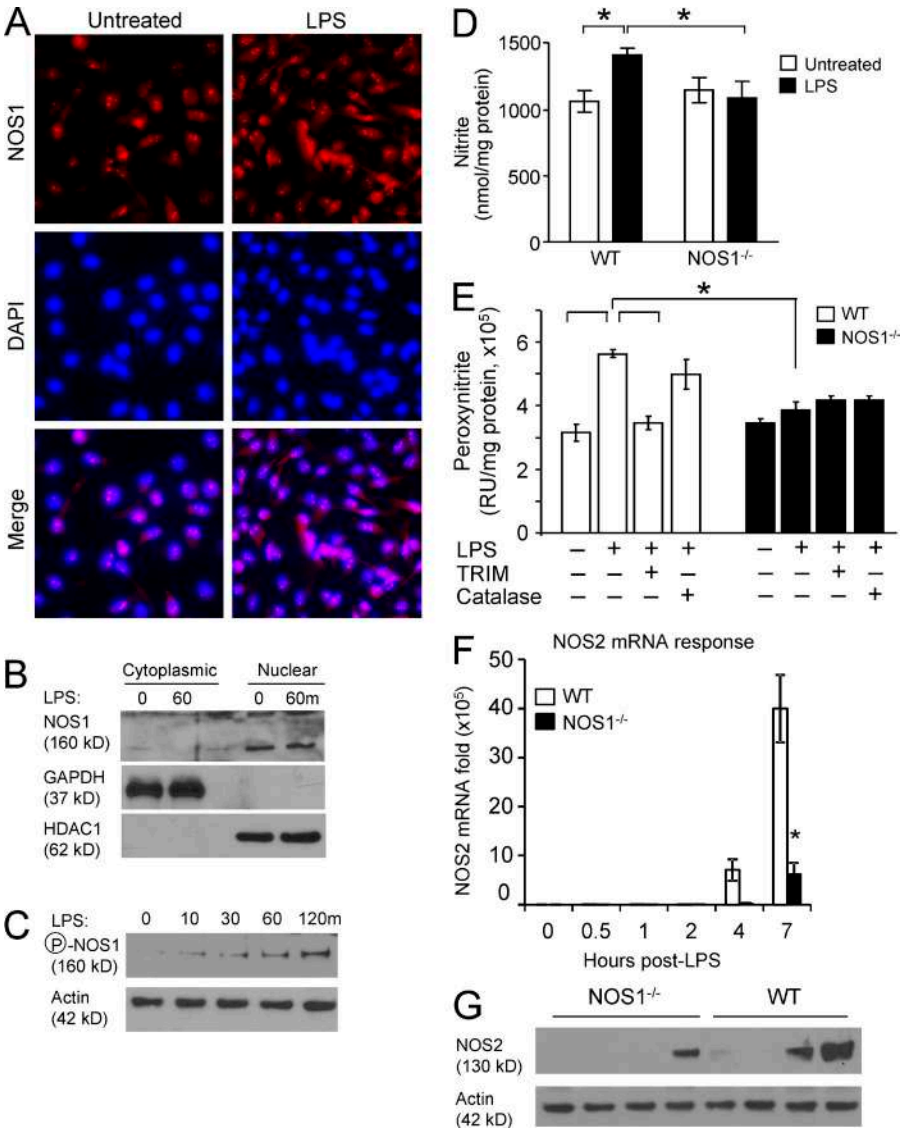

Figure 5. NOS1 localizes to the nuclei of macrophages and is required for rapid NO production after LPS treatment. (A) Nuclear localization of NOS1 was demonstrated in BMDM after fixation and immunostaining for NOS1 (red), nuclei were counterstained with DAPI and representative images from 2 independent experiments are shown (bar, 25 µM). (B) BMDM cytoplasmic and nuclear fractions were immunoblotted to demonstrate the subcellular location of NOS1. GAPDH and HDAC1 serve as controls for subcellular fractionation. (C) NOS1 Serine 1412 phosphorylation, which correlates with enzymatic activation, was assayed by immunoblot of BMDM stimulated with LPS (100 ng/ml) for the indicated time points. Data are representative of three independent experiments. (D) Nitrite accumulation, as an indirect measure of NO production, was detected in the supernatants of WT and *NOS1*$^{-/-}$ BMDM using a Sievers 280i Nitric Oxide Analyzer, before or after LPS (100 ng/ml for 1 h). *, $P < 0.05$. (E) Peroxynitrite production, another indirect measure of NO production, was assayed by incubating WT or *NOS1*$^{-/-}$ BMDM with coumarin-7-boronic acid (10 µM) for 30 min, with or without LPS (100 ng/ml). Fluorescence measurement was performed using HPLC. *, $P < 0.0003$. (F) Quantitative RT-PCR analysis of LPS-induced *NOS2* mRNA and (G) immunoblot analysis of NOS2 protein, from WT and *NOS1*$^{-/-}$ BMDM treated with LPS (250 ng/ml) demonstrates no detection of the inducible NOS (NOS2) at early time points after LPS in BMDM of either genotype. $P < 0.01$ (Student's *t* test). Data are representative of six (D and E) and three (F) independent experiments; all are presented as mean ± SD. Data in B, C, and G are representative of three independent experiments.

by using the fast-releasing NO donor, diethylamine-nonoate (DEANO). Concurrent treatment with DEANO and LPS reversed the degradation of p65 seen in *NOS1*$^{-/-}$ cells, while also promoting the degradation of SOCS1 (Fig. 6 E). These observations demonstrate that a rapid pulse of NO from NOS1 facilitates SOCS1 degradation, leading to stabilization of p65 protein and sustained NF-κB–dependent transcription. To our knowledge, this is the first demonstration of a posttranslational modification of SOCS1 that regulates its ability to suppress NF-κB nuclear activity.

Cys147 and Cys179 are essential for SOCS1 nitrosation and proteasomal degradation

We next sought to determine the exact residues on SOCS1 that are modified by NOS1-derived NO. We used both predictive molecular modeling techniques, followed by functional analysis of individual point mutants of the candidate residues. SOCS1 contains 5 cysteine residues, and we assessed their likelihood for S-nitrosation by in silico docking models (Fig. 7 A). We analyzed the protein sequence and structure of SOCS1 and modeled the predicted accessibility of each cysteine sulfur atom to the nitrogen atom in S-nitrosoglutathione (GSNO) using minimal energy calculations (Fig. 7 B and not depicted). We chose GSNO because it is the likely physiological carrier of reactive NO (Sun et al., 2011; Green et al., 2012). This approach predicted the most susceptible residues to nitrosation were Cys147 and Cys179, which are within the SH2 domain (at the vicinity of the SOCS box) and the SOCS box domain itself (the p65 binding domain), respectively (Fig. 7, A and B). Modification to these domains could explain our observation that NOS1 decreases the binding between SOCS1 and p65 even in the absence of proteasomal degradation. To empirically verify these in silico predictions, we transiently expressed either WT or individual cysteine to serine point mutant constructs

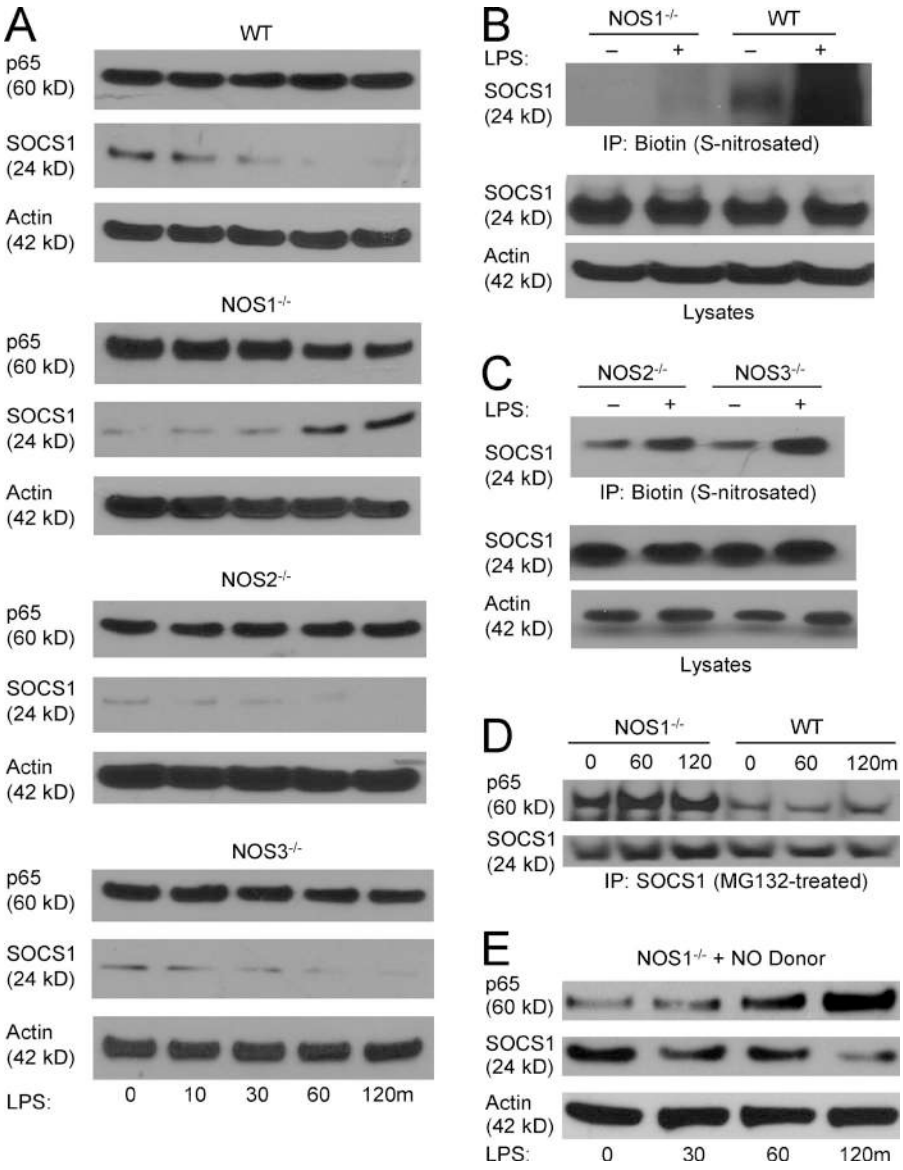

Figure 6. NOS1-derived NO mediates S-nitrosation of SOCS1 and prevents SOCS1-mediated proteasomal degradation of p65. (A) Immunoblot analysis of p65 and SOCS1 in WT, *NOS1*$^{-/-}$, *NOS2*$^{-/-}$, and *NOS3*$^{-/-}$ BMDM treated with LPS (250 ng/ml) for the indicated times. (B) SOCS1 S-nitrosation was detected using the biotin switch method on protein from WT and *NOS1*$^{-/-}$ BMDMs pretreated with MG132 (50 µM) for 1 h before treatment with LPS (250 ng/ml) for the indicated times, followed by immunoblotting for SOCS1. (C) *NOS2*$^{-/-}$ and *NOS3*$^{-/-}$ BMDMs analyzed by biotin switch method, as in B. (D) Co-immunoprecipitation of SOCS1 and p65 in WT and *NOS1*$^{-/-}$ BMDMs, pretreated with MG132 (50 µM, 1 h) before LPS (250 ng/ml) for the indicated time intervals. (E) Immunoblot analysis of p65 and SOCS1 total protein levels in *NOS1*$^{-/-}$ BMDM treated with DEANO (NO donor, 5 µM) and LPS (250 ng/ml). All blots shown are representative of at least two (C and D) or three (A, B, and E) independent experiments.

of SOCS1 in HEK293 cells. Transfected cells were exposed to exogenous NO using DEANO, with or without MG132, to assess the susceptibility of each protein to NO-directed proteasomal degradation. In agreement with our in silico predictions, we determined that although WT SOCS1 protein was degraded upon exposure to NO, C147S and C179S mutants were only minimally affected (Fig. 7, C and D). In contrast, mutations of the three cysteines predicted not to be targets of S-nitrosation (C43S, C78S, and C112S) demonstrated degradation similar to WT SOCS1 (Fig. 7 C). To confirm that this effect was directly correlated with S-nitrosation, we performed a biotin switch assay. Although WT SOCS1 was robustly modified in the presence of the NO donor, S-nitrosation was dampened in the C147S and C179S mutants (Fig. 7 E). These findings demonstrate that the two cysteine residues in SOCS1 closest to the SOCS box are critical for regulating the stability of SOCS1 and its capacity to repress p65-mediated inflammatory transcription. Our results demonstrate that modifications of both Cys147 and Cys179 are required for full S-nitrosation and subsequent degradation of SOCS1.

DISCUSSION

Immunoregulatory functions for NO have long been recognized, owing to the potent induction of the high output, inducible NOS2 isoform associated with the inflammatory response. NO from NOS2 is known to mediate feedback inhibition of proinflammatory signaling pathways, including NF-κB (Peng et al., 1995; Matthews et al., 1996; Togashi et al., 1997; delaTorre et al., 1999; Marshall and Stamler, 2001; Marshall et al., 2004; Reynaert et al., 2004; Kelleher et al., 2007). Although some studies have suggested that lower concentrations of NO from NOS1 can promote inflammation (Porras et al., 2006; Kanwar et al., 2009; Lange et al., 2010; Duma et al., 2011), the mechanism of action for NOS1 has remained obscure. In this study,

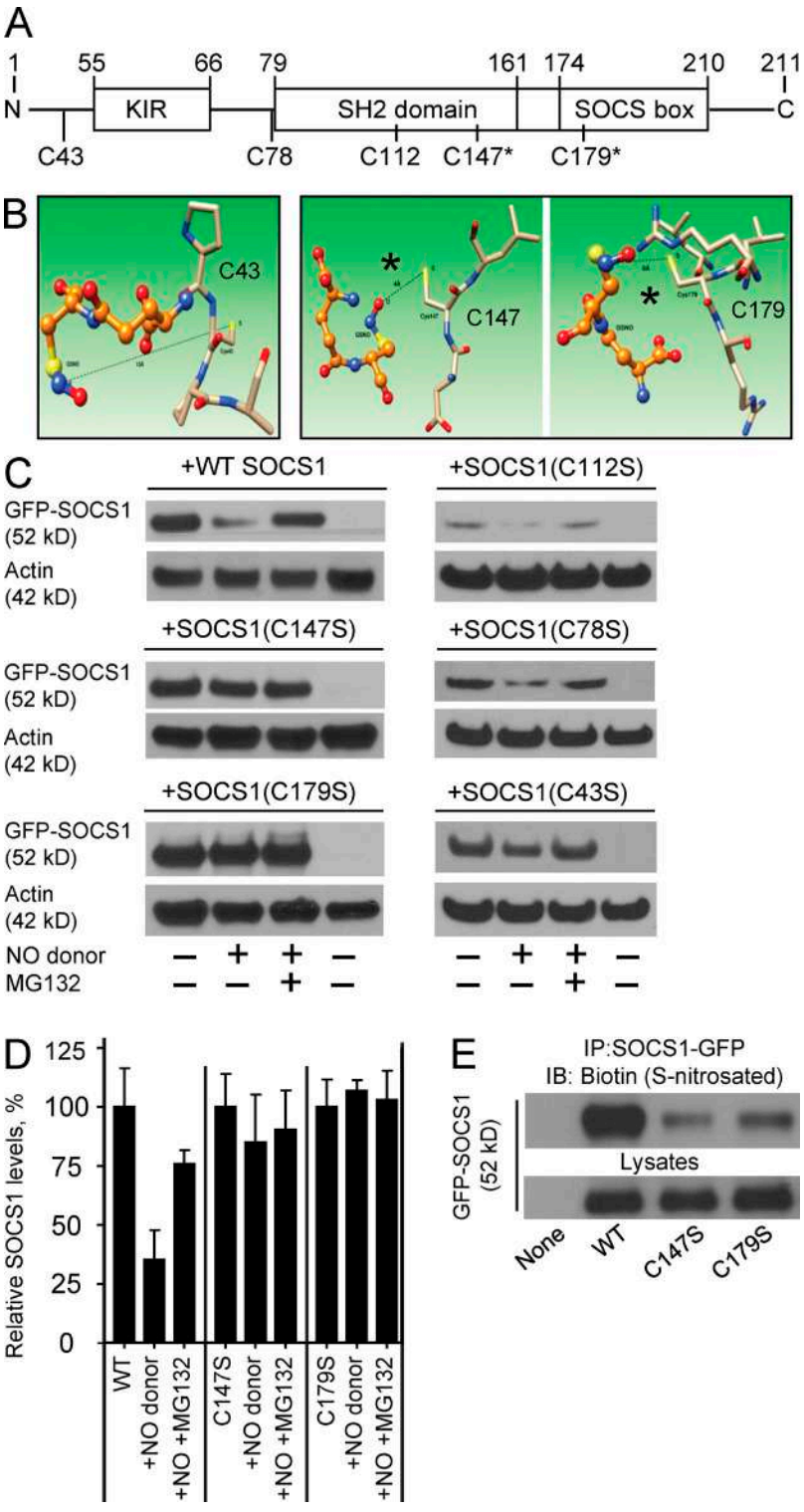

Figure 7. Molecular modeling and functional testing demonstrate that Cys147 and Cys179 of SOCS1 are the targets for S-nitrosation. (A) Protein domain structure of SOCS1 illustrating the positions of all 5 candidate cysteine residues. (B) Molecular modeling was performed to predict the accessibility of cysteine residues of SOCS1 (represented as colored stick atomic models) to the likely transnitrosation donor, GSNO (represented as ball and stick atomic models). The shorter distances between the cysteine sulfur atom and the nitrogen of GSNO are predicted to permit S-nitrosation for Cys147 (4 Å, middle) and Cys179 (6 Å, right), whereas Cys43 (13 Å, left), Cys112 (11 Å, not depicted), and Cys78 (11 Å, not depicted) are predicted to be too far apart to permit the reaction. (C) Representative immunoblots of GFP-tagged constructs of SOCS1 or point mutations of each cysteine (C147S, C179S, C112S, C78S, and C43S) were transfected into HEK293 cells, which were then treated with a 15-min pulse of 20 ng/ml IL-1β. Some of the cells were pretreated with 50 µM proteasome inhibitor for 1 h (MG132 +) and some were treated with 10 µM DEANO for 1 h after IL-1β (NO donor +). Stability of SOCS1 protein levels was determined by immunoblot and (D) quantified relative to β-actin from three independent experiments (mean ± SEM). (E) The capacity of SOCS1 mutants C147S, and C179S for S-nitrosation was compared with WT SOCS1 in transiently transfected HEK293 cells using the biotin switch method. Immunoprecipitates of GFP-SOCS1 variants were assayed for biotin (S-nitrosation), and lysates were immunoblotted for total SOCS1 as control. Data are representative of two independent experiments.

we demonstrate that NO from NOS1 is critical for NF-κB activity, specifically through the S-nitrosation–mediated degradation of SOCS1, which blocks the targeted proteolysis of p65, permitting sustained proinflammatory gene transcription.

We confirmed a physiologically important role for NOS1 in two models of sepsis, a sterile inflammatory model induced by i.p. treatment with LPS, as well as polymicrobial sepsis resulting from CLP. Both treatments resulted in significantly reduced mortality in *NOS1*$^{-/-}$ animals (Fig. 1). This is unique to NOS1 because, consistent with the findings of others, we demonstrate that *NOS2*$^{-/-}$ and *NOS3*$^{-/-}$ mice show increased mortality (Hickey et al., 1997; Wang et al., 2004; Miki et al.,

2005; Duma et al., 2011). Inflammatory cytokines are critical for septic injury, and *NOS1*$^{-/-}$ mice and *NOS1*$^{-/-}$ BMDM both exhibit diminished cytokine responses to LPS treatment (Fig. 2). Indeed, pharmacological inhibition of NOS1 with TRIM replicates these *NOS1*$^{-/-}$ phenotypes. Although TRIM is able to inhibit the activity of NOS2, as well as NOS1, we do not detect any expression of NOS2 at time points where we can detect and inhibit NOS1-dependent, NO-derived products (Fig. 5). Collectively, these findings demonstrate that NOS enzymatic activity, specific to NOS1, is required for the inflammatory injury caused by sepsis.

The variety of the cytokines affected hinted at a defect in the inflammatory signaling pathways downstream of TLR4. We were surprised by the observation that whereas IκB degradation was normal in *NOS1*$^{-/-}$ macrophages, NF-κB–dependent transcription was significantly reduced (Fig. 3). Our findings that other proximal signaling pathways activated by TLR4, ERK1/2, and JNK MAPK activation were intact in *NOS1*$^{-/-}$ cells led us to scrutinize the NF-κB pathway in more detail (unpublished data). We were surprised to find that the levels of p65 protein were significantly decreased in activated *NOS1*$^{-/-}$ macrophages, in clear distinction with WT or *NOS3*$^{-/-}$ cells, which maintained p65 protein (Fig. 4, A and B). We observed that proteasomal inhibition with MG132 could rescue p65 protein levels in *NOS1*$^{-/-}$ cells, and that inhibition of protein synthesis with emetin did not abolish the difference between WT and knockout p65 responses. In addition, we observed no changes in protein levels for the canonical p65 binding partner, NF-κB p50 (Fig. 4 C). Collectively, these findings demonstrate that NOS1-derived NO regulates the specific proteasomal targeting of p65. p50 homodimers can mediate distinct anti-inflammatory transcriptional responses compared with the p65–p50 complex (Driessler et al., 2004). Our studies therefore suggest that in addition to modulating the intensity of the inflammatory response, NOS1-derived NO may influence the quality of the inflammatory response to TLR4 stimulation, as well.

SOCS1, a signaling molecule best known for negative regulation of JAK/STAT signaling, has been reported to mediate ubiquitination of DNA-bound p65, leading to its proteasomal lysis (Ben-Neriah, 2003; Ryo et al., 2003; Strebovsky et al., 2011). This mechanism was consistent with our observations of p65, and indeed, we did find that SOCS1 protein levels were higher in LPS-treated *NOS1*$^{-/-}$ cells (Fig. 6 A). Consistent with this, we used the biotin switch method to find that SOCS1 was S-nitrosated in WT macrophages within 60 min of LPS treatment. Unlike *NOS2*$^{-/-}$ or *NOS3*$^{-/-}$ cells, S-nitrosation at these time points was completely absent in *NOS1*$^{-/-}$ cells (Fig. 6, B and C). Our predictive modeling and functional mutational analysis of SOCS1 identified Cysteine 147 and Cysteine 179 as being required for S-nitrosation and SOCS1 degradation (Fig. 7). We also observed that in the absence of proteasomal degradation, *NOS1*$^{-/-}$ macrophages display reduced binding of SOCS1 and p65 compared with WT (Fig. 6 D). It is possible, therefore, that SOCS1 inhibition may be transient and reversible, or more durable once the SOCS1 protein is degraded. This notion is supported by the finding that although the nitroso modification of both Cys147 or Cy179 residues was required to direct SOCS1 proteolysis, the individual mutants retained a reduced ability to bind to p65 (Fig. 7, C and E; and not depicted).

Unlike other reports that have demonstrated NO can reduce the activity of NF-κB by direct nitrosation as a result of NOS2 activity (Kelleher et al., 2007), we observed that NO generation from NOS1, within 60 min after TLR4 activation, led to stabilization of the p65 transcription factor. This is in agreement with previously reported in vitro observations that NOS1 regulates the DNA binding ability of p65 (Peng et al., 1995; Matthews et al., 1996). We have identified direct nitrosation of SOCS1 as the molecular mechanism for this effect. This extends the importance of SOCS1-mediated regulation of p65, and suggests that the ability to modulate the balance of SOCS1 and p65 through pharmacological targeting of NOS1 could provide important therapeutic interventions to shape the inflammatory responses in a wide range of clinically relevant diseases. Collectively, we find that the anti-inflammatory proteolytic targeting of NF-κB p65 by SOCS1 is an active mechanism during LPS stimulation of macrophages, and that NO, derived uniquely from NOS1, is required to suppress SOCS1 and drive sustained inflammatory transcription.

MATERIALS AND METHODS

Animals and cell culture. Animal handling and experiments were conducted in accordance with the policies of the Animal Care Facility of the University of Illinois at Chicago and the National Institute of Environmental Health Sciences (NIEHS). All animals were acquired from The Jackson Laboratory. *NOS1* knockout mice, *NOS2* knockout mice, and *NOS3* knockout mice were obtained from JAX. WT C57BL/6 animals were used as control. Strain-specific genotyping was performed by Transnetyx Inc. In all experiments, we used 8–12-wk-old male animals. BMDMs were prepared from C57/BL6, *NOS1*$^{-/-}$, *NOS2*$^{-/-}$, or *NOS3*$^{-/-}$ mice (The Jackson Laboratory) by culturing single-cell suspensions of BM for 5–7 d in Dulbecco's minimal essential medium (DMEM) from Invitrogen or RPMI (Gibco) made complete by addition of 10% heat-inactivated FBS (Atlanta Biologicals or Gibco), 100 U/ml penicillin and 100 µg/ml streptomycin from CellGro by Mediatech or 1% (vol/vol) Antibiotic-Antimycotic mix from Life Technologies, with 10–20% L929 cell-conditioned (ATCC) complete DMEM medium. Macrophages were washed and lifted by spraying cells with 1 mM EDTA in 1× PBS from an 18-gauge needle (BD), and then plated for experiments 1–3 d later. RAW264.7 cells stably transfected with the ELAM luciferase reporter (Hume et al., 2001) were cultured in RPMI (Life Technologies) made complete as above. Luciferase expression was assessed by lysing cells (Promega), adding Luciferase Assay Reagent (Promega) and detection using a Wallac Victor2 (PerkinElmer).

In vivo studies. Septic inflammation was induced in mice using two methods. i.p. LPS animals received an intraperitoneal injection of 30 mg/kg LPS (*Escherichia coli*, 0111:B4; Sigma-Aldrich), a dose demonstrating a mortality rate of >80% in C57/BL6 animals. CLP was performed under ketamine/xylazine anesthesia as described previously (Rittirsch et al., 2009). The distal 20% (below the ileocecal valve, ~1 cm from the tip) of the cecum was ligated with a 6–0 suture. The cecum was punctured 4 times with a 20-gauge needle. For survival studies, lethal endpoints were observed for 96 h, at which point all remaining animals were sacrificed. For histopathological observation, animals were sacrificed and lungs were removed 8 h after treatment. Lungs were fixed in 10% neutral buffered formalin, dehydrated, embedded in paraffin, sectioned, and then stained with hematoxylin and eosin (at the facilities of

Research Histology and Tissue Imaging Core [RHTIC], University of Illinois, Chicago, IL). Microvessel K_{fc} was measured to determine the pulmonary microvascular permeability to liquids, as described previously (Vogel et al., 2000). In brief, after standard 30 min equilibration perfusion, the outflow pressure was rapidly elevated by 13 cm H_2O for 20 min and then returned to normal. The changes of lung wet weight reflect net fluid extravasation. At the end of each experiment, lungs were dissected free of nonpulmonary tissue, and lung dry weight was determined. K_{fc} (ml/min/cmH_2O/dry weight [g]) was calculated from the slope of the recorded weight change normalized to the pressure change and to lung dry weight. For some experiments, the NOS1/NOS2 dual inhibitor, 1-(2-trifluoromethylphenyl) imidazole (TRIM; 25 mg/kg, i.p.) was administered 2 h before LPS administration.

For cytokine production analysis, blood samples from 6 mice per phenotype were clotted and centrifuged 2,000 *g* for 20 min, and serum was stored at −80°C until assay. The concentrations of IL-1α, IL-1β, and IL-6 were detected by ELISA Luminex xMAP detection, according to the manufacturer's instructions (EMD Millipore).

HLL transgenic mice (C57B6/DBA background) express Photinus luciferase cDNA under the control of proximal 5′ HIV-LTR promoter. Only 8–12-wk-old males were used in the experiment. Bioluminescence intravital imaging was performed using an IVIS charge-coupled camera (PerkinElmer). 24 h after the indicated treatment, mice were anesthetized by isoflurane, fur was removed from chest and abdomen, 100 µl luciferin (300 mg/ml) was injected i.p. (Caliper Life Sciences), and imaging was performed 10–15 min later. Quantitative analysis was performed by selecting signal over the chest area only, and data were expressed as photons per second.

Nitrite and peroxynitrite measurements. Nitrite, a stable metabolite of NO, was measured in culture supernatants by chemiluminescence. BMDMs were washed twice with HBSS and incubated in serum-free HBSS (Life Technologies) containing 1 mM L-arginine (Sigma-Aldrich) at 37°C, and treated with LPS (*E. coli*, B4:111) for 2 h. After treatment, media was collected, kept ice cold, and centrifuged to remove floating cells. NO concentration in the culture medium was assessed indirectly by measuring NO_{2-} accumulation using a 280i Nitric Oxide Analyzer (Sievers Instruments) and reported as nmol NO per mg protein. Measurement of peroxynitrite production was done using Coumarin-7-boronate (CBA; Sigma-Aldrich). BMDM plated in 6-well plates, either treated with 100 µM TRIM (Sigma-Aldrich) for 1 h or control, were washed twice with DPBS, and incubated in serum-free HBSS buffer containing 20 µM CBA. Cells were then stimulated with LPS (250 ng/ml). Catalase (10 U/ml; Sigma-Aldrich) was also added in the negative control group. After 60 min, media was collected and centrifuged at 3,000 rpm for 5 min. Fluorescence analysis of the oxidation product 7-OH-coumarin (COH) was performed on a Beckman-Coulter HPLC system. Samples (20 µl) were separated on a Synergi-Fusion (250 × 4.6 mm; Phenomenex) using an isocratic elution with 35% vol/vol acetonitrile, at a flow rate of 1 ml/min. Fluorescence was measured using 350 nm (excitation) and 450 nm (emission). Authentic COH solution was injected onto the HPLC to verify the retention time and generate a standard curve.

Confocal analysis. For SOCS1 and p65 staining, BMDMs were plated on coverslips (19-mm diam) and stimulated in 12-well plates. Cells were fixed with 2% paraformaldehyde for 15 min at room temperature and permeabilized for 10 min with ice-cold 100% methanol slowly added to prechilled cells at −20°C. All subsequent steps were conducted at room temperature. The cells were blocked with 5% BSA in 1× PBS for 1 h, and then stained with primary antibodies (mouse anti-SOCS1 and rabbit anti-p65 antibody from Cell Signaling Technology; 1/200 in blocking buffer) for 1 h. After washing with PBS (×5), the cells were stained with Alexa Fluor 568–conjugated goat anti–rabbit IgG and Alexa Fluor 488–conjugated donkey anti–mouse IgG (1/500 in PBS) for 1 h. DAPI was used for nuclear counterstaining according to the manufactorer's protocol. The coverslips were mounted onto glass slides with VECTASHIELD Mounting Media (Vector Laboratories) and analyzed on a LSM 510 META confocal laser scanning microscope (Carl Zeiss) fitted with: 25 mW diode UV laser (DAPI, blue), 1 mW HeNe laser (Alexa Fluor 546, red), 30 mW tunable Ar laser (Alexa Fluor 488, green), and 63×/1.2 Water DIC C-Apochromat objective (UIC imaging core facility). Images were all taken with the same set exposure and processed using LSM software (Carl Zeiss).

mRNA isolation, cDNA synthesis, and real-time PCR. Total RNA was isolated from BMDMs using TRIzol reagent according to the manufacturer's specifications (Invitrogen). cDNA was synthesized using TaqMan RT-PCR kit (Life Technology) according to the manufacturer's specifications. qPCR was performed using Power SYBR Green PCR Master Mix (Applied Biosystems) on a 7500 Real-Time PCR System (Applied Biosystems). The following primer sets (each 5 pmol) were used to amplify cDNA fragments: *TNF* forward primer 5′-TTCGGCTACCCCAAGTTCAT-3′ and reverse primer 5′-CGCACGTAGTTCCGCTTTC-3′; *IL-1*β forward primer 5′-CCATGGCACATTCTGTTCAAA-3′ and reverse primer 5′-GCCCATCAGAGGCAAGGA-3′; *IL6* forward primer 5′-CCACGGCCTTCCCTACTTC-3′ and reverse primer 5′-TTGGGAGTGGTATCCTCTGTGA-3′; *GAPDH* forward primer 5′-GCACAGTCAAGGCCGAGAAT-3′ and reverse primer 5′-GCCTTCTCCATGGTGGTGAA-3′. Cycle threshold (Ct) values were transformed to linear scale ($1/2^{Ct}$), and the resulting data were normalized to GAPDH values for each sample. Data are presented as the percentage of the maximal mRNA response for each dataset. Analysis was performed with Microsoft Excel. To analyze levels of *NOS2* mRNA in BMDM, total mRNA was isolated from 1.2–1.4 × 10^6 BMDM with RNA STAT-60 (Tel-Test, Inc.) according to manufacturer's protocol. 4.6 µg of total mRNA was converted to cDNA using high capacity cDNA RT kit (Applied Biosystems), and 0.46 µg of resulting cDNA was further analyzed by qPCR using Fast SYBR Green Master mix (Applied Biosystems), AB7500 cycler, and the following primers: *NOS2* forward 5′-CAGCTGGGCTGTACAAACCTT-3′; *NOS2* reverse 5′-CATTGGAAGTGAAGCGTTTCG-3′ (de Souza et al., 2013; Shi et al., 2003); *GAPDH* forward 5′-AACGACCCCTTCATTGAC-3′; *GAPDH* reverse 5′-TCCACGACATACTCAGCAC-3′. Ct values were analyzed as above. All values were normalized to the values obtained for *GAPDH* for the same sample to correct for differences in cell number. Results are presented as fold change compared with untreated controls.

Nuclear/cytoplasmic fractionation, cytokine, and p65 DNA binding measurements. The separation of nuclear extracts from cytoplasmic fractions was performed using a Nuclear/Cytosol Extraction kit (BioVision,), Nuclear Extraction kit (Cayman Chemical Company), or NE-PER Nuclear Protein Extraction kit (Thermo Fisher Scientific). Efficient cytoplasmic and nuclear fractionation was confirmed by Western blotting analysis using anti-GAPDH antibody (Cell Signaling Technology) for cytoplasmic fraction and anti-HDAC1 antibody (Santa Cruz Biotechnology, Inc.) for nuclear fraction. NF-κB p65 activity (nuclear DNA binding) was measured with NF-κB (p65) Transcription Factor Assay kit (Cayman Chemical Company) according to the manufacturer's protocol. ∼1 µg of nuclear proteins were analyzed for each condition. Results were obtained with Spectra Max M5^e (Molecular Devices) plate reader (absorbance at 450 nm). The same pools of BMDM were used to measure cytokine levels in parallel to confirm the phenotype, analyzing TNF and IL-1β cytokines with ELISA kits obtained from Thermo Fisher Scientific. Measurements were performed with a Spectra Max M5^e (Molecular Devices) plate reader at 450 and 550 nm.

Immunoblotting, co-immunoprecipitation, and biotin switch assays. For immunoblot analysis, cells were lysed in RIPA buffer (Santa Cruz Biotechnology, Inc.) containing protease and phosphatase inhibitors (Sigma-Aldrich), resolved on NuPAGE 4–12% gels (Novex; Life Technologies), and blotted and probed with the following antibodies against phospho-nNOS-Ser1412, p50, IκBα, GAPDH (Santa Cruz Biotechnology, Inc.), SOCS1 (Abcam), HDAC1, NOS1, GAPDH, β-actin, and anti-p65 (Cell Signaling Technology). After secondary HRP staining (Cell Signaling Technology or Jackson ImmunoResearch Laboratories), chemiluminescence was detected using SuperSignal (Thermo Fisher Scientific) or a luminol-coumeric acid-H_2O_2 chemiluminescence solution, and film (Denville Scientific Inc.) Images were digitally scanned

(HP Officejet J4550 scanner) and analyzed using ImageJ (National Institutes of Health; Schneider et al., 2012). For coimmunoprecipitation, cells were lysed in NP-40 lysis buffer (20 mM Tris-HCL, pH 8.0, 137 mM NaCl, 10% glycerol, 1% NP-40, 2 mM EDTA) with protease inhibitors. Protein concentration was normalized using the BCA assay (Bio-Rad Laboratories). 100 µg of protein lysate was incubated with mouse anti-SOCS1 antibody (Invitrogen) plus protein A/G agarose beads (Santa Cruz Biotechnology, Inc.) overnight, rotating at 4°C. Beads were washed 4× with lysis buffer and protein was analyzed by immunoblot. Biotin-switch assays were conducted using the S-nitrosylated Protein Detection kit (Cayman Chemicals) according to the manufacturer's instructions. Differentiated BMDM were pretreated with MG132 (50 µM) for 1 h and stimulated with LPS (250 ng/ml) for 30 min. S-nitrosated proteins, isolated from an equal number of cells, were precipitated using streptavidin Dynabeads (M-280 Streptavidin; Invitrogen), resolved by NuPAGE 4–12% gels (Novex; Life Technologies) and immunoblotted with either peroxidase-conjugated anti-SOCS1 antibody (1:100; Cell Signaling Technology) or rabbit anti-SOCS1 antibody (1:1,000; Abcam), followed by HRP-conjugated secondary antibody (anti–rabbit; Jackson ImmunoResearch Laboratories).

Expression of GFP-tagged SOCS1 and cysteine mutants in HEK293 cells. HEK293 cells were maintained in complete DMEM. Cells were transiently transfected with pCMV6-AC-GFPVector (OriGene), which expresses SOCS1 (mouse; available from GenBank under accession no. NM_009896.2) driven by the constitutive CMV promoter, using Lipofectamine 2000 reagent according to the manufacturer's protocol. Cysteine mutations (C147S, C179S, C43S, C78S and C112S) were introduced in SOCS1 ORF (GenScript USA Inc.). HEK293 cells were stimulated with a 15 min pulse of 20 ng/ml IL-1β (Prospec Inc.) and treated with 10 µM DEA NONOate (DEANO) for 1 h (Alexis Biochemicals). Diethylamine NO (DEANO) is a member of the NONOate class NO donors. At 37°C, pH 7.4, it generates NO spontaneously with a half-life of 2.1 min (Schödel et al., 2009). Total SOCS1 and corresponding p65 protein level was also determined in the presence and absence of 50 µM MG132 (Sigma-Aldrich) to inhibit proteasomal lysis.

Molecular modeling and computational docking. The 3-dimensional structure of SOCS1 region (residues 65–212) was available from Protein Model Port, while a model of the N terminus (residues 1–64) was constructed using the I-Tasser modeling server. Ramachandran plot analysis was done using SAVES server to test the model quality. The 3-dimensional conformer of the substrate S-nitrosylated glutathione (GSNO; CID_104858) was initially retrieved from Pubchem compound search. The Accelrys discovery studio program (Discovery Studio Modeling Environment; Release 4.0; Accelrys Software Inc.) was used to energy minimize the structure using CHARMM force field parameters. Charges on the NO-Cys were then manually implemented as reported in a recently published study (Han, 2008). GSNO was then exported to Mcule docking for docking calculations. Mcule utilizes the docking calculations based on program AutoDockVina. The preparation of protein and substrate file was done according to the standard AutoDock procedure. In brief, including conversion of input ligands defined by mcule IDs, SMILES, or InChI strings to 2D MOL, generation of defined stereoisomers, conversion of ligand 2D MOL to 3D MOL, conversion of ligand 3D MOL to PDBQT, preparation of docking targets and finally docking. Out of the best four docking poses the top scoring one was analyzed further. Castp server was used for protein pocket detection. The hydrophobicity index for the pocket was calculated according to the Kyte-Doolittle scale (Kyte and Doolittle, 1982) using the Protein GRAVY module of the Sequence Manipulation Suite server.

Statistical analyses. Statistical analyses were performed using Microsoft Excel or Prism (GraphPad). Significance was assessed using two-tailed Student's *t* test, Anova two-way test with Bonferroni post-test, or Fisher's exact test. All data are representative of at least two independent experiments and error refers to standard deviation unless otherwise stated.

The authors are indebted to Ms. Mary Maliakal for preliminary work on NOS1 regulation of p65 phosphorylation.

This work was sponsored by the American Heart Association, Scientist Development Grants nos. 09SDG2250933 and 13GRNT16400010; and Department of Defense grant W911NF-12-1-0493/61758-LS to M.G. Bonini.

The authors declare no competing financial interests.

Submitted: 7 April 2014
Accepted: 6 August 2015

REFERENCES

Aktan, F. 2004. iNOS-mediated nitric oxide production and its regulation. *Life Sci.* 75:639–653. http://dx.doi.org/10.1016/j.lfs.2003.10.042

Alcamo, E., J.P. Mizgerd, B.H. Horwitz, R. Bronson, A.A. Beg, M. Scott, C.M. Doerschuk, R.O. Hynes, and D. Baltimore. 2001. Targeted mutation of TNF receptor I rescues the RelA-deficient mouse and reveals a critical role for NF-kappa B in leukocyte recruitment. *J. Immunol.* 167:1592–1600. http://dx.doi.org/10.4049/jimmunol.167.3.1592

Badrichani, A.Z., D.M. Stroka, G. Bilbao, D.T. Curiel, F.H. Bach, and C. Ferran. 1999. Bcl-2 and Bcl-XL serve an anti-inflammatory function in endothelial cells through inhibition of NF-kappaB. *J. Clin. Invest.* 103:543–553. http://dx.doi.org/10.1172/JCI2517

Baetz, A., M. Frey, K. Heeg, and A.H. Dalpke. 2004. Suppressor of cytokine signaling (SOCS) proteins indirectly regulate toll-like receptor signaling in innate immune cells. *J. Biol. Chem.* 279:54708–54715. http://dx.doi.org/10.1074/jbc.M410992200

Baltimore, D. 2011. NF-κB is 25. *Nat. Immunol.* 12:683–685. http://dx.doi.org/10.1038/ni.2072

Basak, S., H. Kim, J.D. Kearns, V. Tergaonkar, E. O'Dea, S.L. Werner, C.A. Benedict, C.F. Ware, G. Ghosh, I.M. Verma, and A. Hoffmann. 2007. A fourth IkappaB protein within the NF-kappaB signaling module. *Cell.* 128:369–381. http://dx.doi.org/10.1016/j.cell.2006.12.033

Ben-Neriah, Y. 2003. Pinning NF-kappaB to the nucleus. *Mol. Cell.* 12:1344–1345. http://dx.doi.org/10.1016/S1097-2765(03)00493-3

Block, M.L., and J.S. Hong. 2005. Microglia and inflammation-mediated neurodegeneration: multiple triggers with a common mechanism. *Prog. Neurobiol.* 76:77–98. http://dx.doi.org/10.1016/j.pneurobio.2005.06.004

Bowie, A., and L.A. O'Neill. 2000. Oxidative stress and nuclear factor-kappaB activation: a reassessment of the evidence in the light of recent discoveries. *Biochem. Pharmacol.* 59:13–23. http://dx.doi.org/10.1016/S0006-2952(99)00296-8

Bubici, C., S. Papa, K. Dean, and G. Franzoso. 2006. Mutual cross-talk between reactive oxygen species and nuclear factor-kappa B: molecular basis and biological significance. *Oncogene.* 25:6731–6748. http://dx.doi.org/10.1038/sj.onc.1209936

de Souza, K.P., E.G. Silva, E.S. de Oliveira Rocha, L.B. Figueiredo, C.M. de Almeida-Leite, R.M. Arantes, J. de Assis Silva Gomes, G.P. Ferreira, J.G. de Oliveira, E.G. Kroon, and M.A. Campos. 2013. Nitric oxide synthase expression correlates with death in an experimental mouse model of dengue with CNS involvement. *Virol. J.* 10:267. http://dx.doi.org/10.1186/1743-422X-10-26

delaTorre, A., R.A. Schroeder, C. Punzalan, and P.C. Kuo. 1999. Endotoxin-mediated S-nitrosylation of p50 alters NF-kappa B-dependent gene transcription in ANA-1 murine macrophages. *J. Immunol.* 162:4101–4108.

Dixon, B. 2004. The role of microvascular thrombosis in sepsis. *Anaesth. Intensive Care.* 32:619–629.

Dombrovskiy, V.Y., A.A. Martin, J. Sunderram, and H.L. Paz. 2007. Rapid increase in hospitalization and mortality rates for severe sepsis in the United States: a trend analysis from 1993 to 2003. *Crit. Care Med.* 35:1244–1250. http://dx.doi.org/10.1097/01.CCM.0000261890.41311.E9

Driessler, F., K. Venstrom, R. Sabat, K. Asadullah, and A.J. Schottelius. 2004. Molecular mechanisms of interleukin-10-mediated inhibition of NF-kappaB activity: a role for p50. *Clin. Exp. Immunol.* 135:64–73. http://dx.doi.org/10.1111/j.1365-2249.2004.02342.x

Duma, D., D. Fernandes, M.G. Bonini, K. Stadler, R.P. Mason, and J. Assreuy. 2011. NOS-1-derived NO is an essential triggering signal for the development of systemic inflammatory responses. *Eur. J. Pharmacol.* 668:285–292. http://dx.doi.org/10.1016/j.ejphar.2011.05.065

Edgley, A.J., H. Krum, and D.J. Kelly. 2012. Targeting fibrosis for the treatment of heart failure: a role for transforming growth factor-β. *Cardiovasc Ther.* 30:e30–e40. http://dx.doi.org/10.1111/j.1755-5922.2010.00228.x

Fieren, M.W. 2012. The local inflammatory responses to infection of the peritoneal cavity in humans: their regulation by cytokines, macrophages, and other leukocytes. *Mediators Inflamm.* 2012:976241. http://dx.doi.org/10.1155/2012/976241

Gantner, B.N., R.M. Simmons, S.J. Canavera, S. Akira, and D.M. Underhill. 2003. Collaborative induction of inflammatory responses by dectin-1 and Toll-like receptor 2. *J. Exp. Med.* 197:1107–1117. http://dx.doi.org/10.1084/jem.20021787

Geng, H., T. Wittwer, O. Dittrich-Breiholz, M. Kracht, and M.L. Schmitz. 2009. Phosphorylation of NF-kappaB p65 at Ser468 controls its COMMD1-dependent ubiquitination and target gene-specific proteasomal elimination. *EMBO Rep.* 10:381–386. http://dx.doi.org/10.1038/embor.2009.10

Gingras, S., E. Parganas, A. de Pauw, J.N. Ihle, and P.J. Murray. 2004. Re-examination of the role of suppressor of cytokine signaling 1 (SOCS1) in the regulation of toll-like receptor signaling. *J. Biol. Chem.* 279:54702–54707. http://dx.doi.org/10.1074/jbc.M411043200

Green, L.S., L.E. Chun, A.K. Patton, X. Sun, G.J. Rosenthal, and J.P. Richards. 2012. Mechanism of inhibition for N6022, a first-in-class drug targeting S-nitrosoglutathione reductase. *Biochemistry.* 51:2157–2168. http://dx.doi.org/10.1021/bi201785u

Grollman, A.P. 1968. Inhibitors of protein biosynthesis. V. Effects of emetine on protein and nucleic acid biosynthesis in HeLa cells. *J. Biol. Chem.* 243:4089–4094.

Han, S. 2008. Force field parameters for S-nitrosocysteine and molecular dynamics simulations of S-nitrosated thioredoxin. *Biochem. Biophys. Res. Commun.* 377:612–616. http://dx.doi.org/10.1016/j.bbrc.2008.10.017

Handy, R.L., P. Wallace, Z.A. Gaffen, K.J. Whitehead, and P.K. Moore. 1995. The antinociceptive effect of 1-(2-trifluoromethylphenyl) imidazole (TRIM), a potent inhibitor of neuronal nitric oxide synthase in vitro, in the mouse. *Br. J. Pharmacol.* 116:2349–2350. http://dx.doi.org/10.1111/j.1476-5381.1995.tb15078.x

Hickey, M.J., K.A. Sharkey, E.G. Sihota, P.H. Reinhardt, J.D. Macmicking, C. Nathan, and P. Kubes. 1997. Inducible nitric oxide synthase-deficient mice have enhanced leukocyte-endothelium interactions in endotoxemia. *FASEB J.* 11:955–964.

Huang, Z., F.W. Hoffmann, J.D. Fay, A.C. Hashimoto, M.L. Chapagain, P.H. Kaufusi, and P.R. Hoffmann. 2012. Stimulation of unprimed macrophages with immune complexes triggers a low output of nitric oxide by calcium-dependent neuronal nitric-oxide synthase. *J. Biol. Chem.* 287:4492–4502. http://dx.doi.org/10.1074/jbc.M111.315598

Hume, D.A., D.M. Underhill, M.J. Sweet, A.O. Ozinsky, F.Y. Liew, and A. Aderem. 2001. Macrophages exposed continuously to lipopolysaccharide and other agonists that act via toll-like receptors exhibit a sustained and additive activation state. *BMC Immunol.* 2:11. http://dx.doi.org/10.1186/1471-2172-2-11

Jacobs, M.D., and S.C. Harrison. 1998. Structure of an IkappaBalpha/NF-kappaB complex. *Cell.* 95:749–758. http://dx.doi.org/10.1016/S0092-8674(00)81698-0

Jacobson, J.R., and K.G. Birukov. 2009. Activation of NFkB and coagulation in lung injury by hyperoxia and excessive mechanical ventilation: one more reason "low and slow" is the way to go? *Transl. Res.* 154:219–221. http://dx.doi.org/10.1016/j.trsl.2009.07.012

Javaid, K., A. Rahman, K.N. Anwar, R.S. Frey, R.D. Minshall, and A.B. Malik. 2003. Tumor necrosis factor-alpha induces early-onset endothelial adhesivity by protein kinase Czeta-dependent activation of intercellular adhesion molecule-1. *Circ. Res.* 92:1089–1097. http://dx.doi.org/10.1161/01.RES.0000072971.88704.CB

Jeon, Y.J., S.H. Han, J.S. Kang, W.S. Koh, and K.H. Yang. 1999. Acetylaminofluorene inhibits nitric oxide production in LPS-stimulated RAW 264.7 cells by blocking NF-kappa B/Rel activation. *Toxicol. Lett.* 104:195–202. http://dx.doi.org/10.1016/S0378-4274(98)00372-5

Kanwar, J.R., R.K. Kanwar, H. Burrow, and S. Baratchi. 2009. Recent advances on the roles of NO in cancer and chronic inflammatory disorders. *Curr. Med. Chem.* 16:2373–2394. http://dx.doi.org/10.2174/092986709788682155

Kelleher, Z.T., A. Matsumoto, J.S. Stamler, and H.E. Marshall. 2007. NOS2 regulation of NF-kappaB by S-nitrosylation of p65. *J. Biol. Chem.* 282:30667–30672. http://dx.doi.org/10.1074/jbc.M705929200

Kinjyo, I., T. Hanada, K. Inagaki-Ohara, H. Mori, D. Aki, M. Ohishi, H. Yoshida, M. Kubo, and A. Yoshimura. 2002. SOCS1/JAB is a negative regulator of LPS-induced macrophage activation. *Immunity.* 17:583–591. http://dx.doi.org/10.1016/S1074-7613(02)00446-6

Knowles, R.G., and S. Moncada. 1994. Nitric oxide synthases in mammals. *Biochem. J.* 298:249–258. http://dx.doi.org/10.1042/bj2980249

Koelink, P.J., S.A. Overbeek, S. Braber, P. de Kruijf, G. Folkerts, M.J. Smit, and A.D. Kraneveld. 2012. Targeting chemokine receptors in chronic inflammatory diseases: an extensive review. *Pharmacol. Ther.* 133:1–18. http://dx.doi.org/10.1016/j.pharmthera.2011.06.008

Kyte, J., and R.F. Doolittle. 1982. A simple method for displaying the hydropathic character of a protein. *J. Mol. Biol.* 157:105–132. http://dx.doi.org/10.1016/0022-2836(82)90515-0

Lange, M., Y. Nakano, D.L. Traber, A. Hamahata, A. Esechie, C. Jonkam, K. Bansal, L.D. Traber, and P. Enkhbaatar. 2010. Role of different nitric oxide synthase isoforms in a murine model of acute lung injury and sepsis. *Biochem. Biophys. Res. Commun.* 399:286–291. http://dx.doi.org/10.1016/j.bbrc.2010.07.071

Lawrence, T. 2009. The nuclear factor NF-kappaB pathway in inflammation. *Cold Spring Harb. Perspect. Biol.* 1:a001651. http://dx.doi.org/10.1101/cshperspect.a001651

Li, N., S.I. Grivennikov, and M. Karin. 2011. The unholy trinity: inflammation, cytokines, and STAT3 shape the cancer microenvironment. *Cancer Cell.* 19:429–431. http://dx.doi.org/10.1016/j.ccr.2011.03.018

Lin, Y.C., G.D. Huang, C.W. Hsieh, and B.S. Wung. 2012. The glutathionylation of p65 modulates NF-κB activity in 15-deoxy-$\Delta^{12,14}$-prostaglandin J_2-treated endothelial cells. *Free Radic. Biol. Med.* 52:1844–1853. http://dx.doi.org/10.1016/j.freeradbiomed.2012.02.028

Linossi, E.M., and S.E. Nicholson. 2012. The SOCS box-adapting proteins for ubiquitination and proteasomal degradation. *IUBMB Life.* 64:316–323. http://dx.doi.org/10.1002/iub.1011

Liu, Y. 2011. Cellular and molecular mechanisms of renal fibrosis. *Nat. Rev. Nephrol.* 7:684–696. http://dx.doi.org/10.1038/nrneph.2011.149

Ma, A., and B.A. Malynn. 2012. A20: linking a complex regulator of ubiquitylation to immunity and human disease. *Nat. Rev. Immunol.* 12:774–785. http://dx.doi.org/10.1038/nri3313

MacMicking, J., Q.W. Xie, and C. Nathan. 1997. Nitric oxide and macrophage function. *Annu. Rev. Immunol.* 15:323–350. http://dx.doi.org/10.1146/annurev.immunol.15.1.323

Marshall, H.E., and J.S. Stamler. 2001. Inhibition of NF-kappa B by S-nitrosylation. *Biochemistry.* 40:1688–1693. http://dx.doi.org/10.1021/bi002239y

Marshall, H.E., D.T. Hess, and J.S. Stamler. 2004. S-nitrosylation: physiological regulation of NF-kappaB. *Proc. Natl. Acad. Sci. USA.* 101:8841–8842. http://dx.doi.org/10.1073/pnas.0403034101

Matthay, M.A., and R.L. Zemans. 2011. The acute respiratory distress syndrome: pathogenesis and treatment. *Annu. Rev. Pathol.* 6:147–163. http://dx.doi.org/10.1146/annurev-pathol-011110-130158

Matthews, J.R., C.H. Botting, M. Panico, H.R. Morris, and R.T. Hay. 1996. Inhibition of NF-kappaB DNA binding by nitric oxide. *Nucleic Acids Res.* 24:2236–2242. http://dx.doi.org/10.1093/nar/24.12.2236

Mattioli, I., H. Geng, A. Sebald, M. Hodel, C. Bucher, M. Kracht, and M.L. Schmitz. 2006. Inducible phosphorylation of NF-kappa B p65 at serine 468 by T cell costimulation is mediated by IKK epsilon. *J. Biol. Chem.* 281:6175–6183. http://dx.doi.org/10.1074/jbc.M508045200

Miki, S., N. Takeyama, T. Tanaka, and T. Nakatani. 2005. Immune dysfunction in endotoxicosis: role of nitric oxide produced by inducible nitric oxide synthase. *Crit. Care Med.* 33:716–720. http://dx.doi.org/10.1097/01.CCM.0000159200.69314.3A

Nacher, M., and A. Hidalgo. 2011. Fire within the vessels: interactions between blood cells and inflammatory vascular injury. *Front Biosci (Schol Ed).* 3:1089–1100. http://dx.doi.org/10.2741/213

Nakagawa, R., T. Naka, H. Tsutsui, M. Fujimoto, A. Kimura, T. Abe, E. Seki, S. Sato, O. Takeuchi, K. Takeda, et al. 2002. SOCS-1 participates in negative regulation of LPS responses. *Immunity.* 17:677–687. http://dx.doi.org/10.1016/S1074-7613(02)00449-1

Nicholas, C., S. Batra, M.A. Vargo, O.H. Voss, M.A. Gavrilin, M.D. Wewers, D.C. Guttridge, E. Grotewold, and A.I. Doseff. 2007. Apigenin blocks lipopolysaccharide-induced lethality in vivo and proinflammatory cytokines expression by inactivating NF-kappaB through the suppression of p65 phosphorylation. *J. Immunol.* 179:7121–7127. http://dx.doi.org/10.4049/jimmunol.179.10.7121

Panettieri, R.A. Jr., M.I. Kotlikoff, W.T. Gerthoffer, M.B. Hershenson, P.G. Woodruff, I.P. Hall, and S. Banks-Schlegel. National Heart, Lung, and Blood Institute. 2008. Airway smooth muscle in bronchial tone, inflammation, and remodeling: basic knowledge to clinical relevance. *Am. J. Respir. Crit. Care Med.* 177:248–252. http://dx.doi.org/10.1164/rccm.200708-1217PP

Park, S.H., K.E. Kim, H.Y. Hwang, and T.Y. Kim. 2003. Regulatory effect of SOCS on NF-kappaB activity in murine monocytes/macrophages. *DNA Cell Biol.* 22:131–139. http://dx.doi.org/10.1089/104454903321515931

Parsons, P.E., M.D. Eisner, B.T. Thompson, M.A. Matthay, M. Ancukiewicz, G.R. Bernard, and A.P. Wheeler. NHLBI Acute Respiratory Distress Syndrome Clinical Trials Network. 2005. Lower tidal volume ventilation and plasma cytokine markers of inflammation in patients with acute lung injury. *Crit. Care Med.* 33:1–6, discussion :230–232. http://dx.doi.org/10.1097/01.CCM.0000149854.61192.DC

Peng, H.B., P. Libby, and J.K. Liao. 1995. Induction and stabilization of I kappa B alpha by nitric oxide mediates inhibition of NF-kappa B. *J. Biol. Chem.* 270:14214–14219. http://dx.doi.org/10.1074/jbc.270.23.14214

Pittet, L.A., L.J. Quinton, K. Yamamoto, B.E. Robson, J.D. Ferrari, H. Algül, R.M. Schmid, and J.P. Mizgerd. 2011. Earliest innate immune responses require macrophage RelA during pneumococcal pneumonia. *Am. J. Respir. Cell Mol. Biol.* 45:573–581. http://dx.doi.org/10.1165/rcmb.2010-0210OC

Porras, M., M.T. Martín, R. Torres, and P. Vergara. 2006. Cyclical upregulated iNOS and long-term downregulated nNOS are the bases for relapse and quiescent phases in a rat model of IBD. *Am. J. Physiol. Gastrointest. Liver Physiol.* 290:G423–G430. http://dx.doi.org/10.1152/ajpgi.00323.2005

Reynaert, N.L., K. Ckless, S.H. Korn, N. Vos, A.S. Guala, E.F. Wouters, A. van der Vliet, and Y.M. Janssen-Heininger. 2004. Nitric oxide represses inhibitory kappaB kinase through S-nitrosylation. *Proc. Natl. Acad. Sci. USA.* 101:8945–8950. http://dx.doi.org/10.1073/pnas.0400588101

Rittirsch, D., M.S. Huber-Lang, M.A. Flierl, and P.A. Ward. 2009. Immunodesign of experimental sepsis by cecal ligation and puncture. *Nat. Protoc.* 4:31–36. http://dx.doi.org/10.1038/nprot.2008.214

Rossi, B., S. Angiari, E. Zenaro, S.L. Budui, and G. Constantin. 2011. Vascular inflammation in central nervous system diseases: adhesion receptors controlling leukocyte-endothelial interactions. *J. Leukoc. Biol.* 89:539–556. http://dx.doi.org/10.1189/jlb.0710432

Ruland, J. 2011. Return to homeostasis: downregulation of NF-κB responses. *Nat. Immunol.* 12:709–714. http://dx.doi.org/10.1038/ni.2055

Ryo, A., F. Suizu, Y. Yoshida, K. Perrem, Y.C. Liou, G. Wulf, R. Rottapel, S. Yamaoka, and K.P. Lu. 2003. Regulation of NF-kappaB signaling by Pin1-dependent prolyl isomerization and ubiquitin-mediated proteolysis of p65/RelA. *Mol. Cell.* 12:1413–1426. http://dx.doi.org/10.1016/S1097-2765(03)00490-8

Sabatel, H., E. Di Valentin, G. Gloire, F. Dequiedt, J. Piette, and Y. Habraken. 2012. Phosphorylation of p65(RelA) on Ser(547) by ATM represses NF-κB-dependent transcription of specific genes after genotoxic stress. *PLoS ONE.* 7:e38246. http://dx.doi.org/10.1371/journal.pone.0038246

Sadik, C.D., N.D. Kim, and A.D. Luster. 2011. Neutrophils cascading their way to inflammation. *Trends Immunol.* 32:452–460. http://dx.doi.org/10.1016/j.it.2011.06.008

Sadikot, R.T., E.D. Jansen, T.R. Blackwell, O. Zoia, F. Yull, J.W. Christman, and T.S. Blackwell. 2001. High-dose dexamethasone accentuates nuclear factor-kappa b activation in endotoxin-treated mice. *Am. J. Respir. Crit. Care Med.* 164:873–878. http://dx.doi.org/10.1164/ajrccm.164.5.2008059

Saluja, R., R. Saini, K. Mitra, V.K. Bajpai, and M. Dikshit. 2010. Ultrastructural immunogold localization of nitric oxide synthase isoforms in rat and human eosinophils. *Cell Tissue Res.* 340:381–388. http://dx.doi.org/10.1007/s00441-010-0947-y

Schneider, C.A., W.S. Rasband, and K.W. Eliceiri. 2012. NIH Image to ImageJ: 25 years of image analysis. *Nat. Methods.* 9:671–675. http://dx.doi.org/10.1038/nmeth.2089

Schödel, J., P. Padmapriya, A. Marx, P.L. Huang, G. Ertl, and P.J. Kuhlencordt. 2009. Expression of neuronal nitric oxide synthase splice variants in atherosclerotic plaques of apoE knockout mice. *Atherosclerosis.* 206:383–389. http://dx.doi.org/10.1016/j.atherosclerosis.2009.02.033

Shi, L., Y.J. Jung, S. Tyagi, M.L. Gennaro, and R.J. North. 2003. Expression of Th1-mediated immunity in mouse lungs induces a Mycobacterium tuberculosis transcription pattern characteristic of nonreplicating persistence. *Proc. Natl. Acad. Sci. USA.* 100:241–246. http://dx.doi.org/10.1073/pnas.0136863100

Strebovsky, J., P. Walker, R. Lang, and A.H. Dalpke. 2011. Suppressor of cytokine signaling 1 (SOCS1) limits NFkappaB signaling by decreasing p65 stability within the cell nucleus. *FASEB J.* 25:863–874. http://dx.doi.org/10.1096/fj.10-170597

Summers deLuca, L., and J.L. Gommerman. 2012. Fine-tuning of dendritic cell biology by the TNF superfamily. *Nat. Rev. Immunol.* 12:339–351. http://dx.doi.org/10.1038/nri3193

Sun, B., and M. Karin. 2012. Obesity, inflammation, and liver cancer. *J. Hepatol.* 56:704–713. http://dx.doi.org/10.1016/j.jhep.2011.09.020

Sun, X., J.W. Wasley, J. Qiu, J.P. Blonder, A.M. Stout, L.S. Green, S.A. Strong, D.B. Colagiovanni, J.P. Richards, S.C. Mutka, et al. 2011. Discovery of s-nitrosoglutathione reductase inhibitors: potential agents for the treatment of asthma and other inflammatory diseases. *ACS Med Chem Lett.* 2:402–406. http://dx.doi.org/10.1021/ml200045s

Takizawa, H., S. Boettcher, and M.G. Manz. 2012. Demand-adapted regulation of early hematopoiesis in infection and inflammation. *Blood.* 119:2991–3002. http://dx.doi.org/10.1182/blood-2011-12-380113

Tiruppathi, C., J. Shimizu, K. Miyawaki-Shimizu, S.M. Vogel, A.M. Bair, R.D. Minshall, D. Predescu, and A.B. Malik. 2008. Role of NF-kappaB-dependent caveolin-1 expression in the mechanism of increased endothelial permeability induced by lipopolysaccharide. *J. Biol. Chem.* 283:4210–4218. http://dx.doi.org/10.1074/jbc.M703153200

Togashi, H., M. Sasaki, E. Frohman, E. Taira, R.R. Ratan, T.M. Dawson, and V.L. Dawson. 1997. Neuronal (type I) nitric oxide synthase regulates nuclear factor kappaB activity and immunologic (type II) nitric oxide synthase expression. *Proc. Natl. Acad. Sci. USA.* 94:2676–2680. http://dx.doi.org/10.1073/pnas.94.6.2676

Vallabhapurapu, S., and M. Karin. 2009. Regulation and function of NF-kappaB transcription factors in the immune system. *Annu. Rev. Immunol.* 27:693–733. http://dx.doi.org/10.1146/annurev.immunol.021908.132641

Vanden Berghe, W., K. De Bosscher, E. Boone, S. Plaisance, and G. Haegeman. 1999. The nuclear factor-kappaB engages CBP/p300 and histone acetyltransferase activity for transcriptional activation of the interleukin-6 gene promoter. *J. Biol. Chem.* 274:32091–32098. http://dx.doi.org/10.1074/jbc.274.45.32091

Villanueva, C., and C. Giulivi. 2010. Subcellular and cellular locations of nitric oxide synthase isoforms as determinants of health and disease. *Free Radic. Biol. Med.* 49:307–316. http://dx.doi.org/10.1016/j.freeradbiomed.2010.04.004

Vogel, S.M., X. Gao, D. Mehta, R.D. Ye, T.A. John, P. Andrade-Gordon, C. Tiruppathi, and A.B. Malik. 2000. Abrogation of thrombin-induced increase in pulmonary microvascular permeability in PAR-1 knockout mice. *Physiol. Genomics.* 4:137–145.

Wang, W., A. Mitra, B. Poole, S. Falk, M.S. Lucia, S. Tayal, and R. Schrier. 2004. Endothelial nitric oxide synthase-deficient mice exhibit increased susceptibility to endotoxin-induced acute renal failure. *Am. J. Physiol. Renal Physiol.* 287:F1044–F1048. http://dx.doi.org/10.1152/ajprenal.00136.2004

Xia, Y., M.E. Pauza, L. Feng, and D. Lo. 1997. RelB regulation of chemokine expression modulates local inflammation. *Am. J. Pathol.* 151:375–387.

Yuan, Z., B. Liu, L. Yuan, Y. Zhang, X. Dong, and J. Lu. 2004. Evidence of nuclear localization of neuronal nitric oxide synthase in cultured astrocytes of rats. *Life Sci.* 74:3199–3209. http://dx.doi.org/10.1016/j.lfs.2003.10.037